

STUDY OF TORSIONAL BEHAVIOUR OF RECTANGULAR REINFORCED CONCRETE BEAMS WRAPPED WITH GFRP

*A thesis
Submitted by*

**Chhabirani Tudu
(210CE2277)**

*In partial fulfillment of the requirements
for the award of the degree of*

**Master of Technology
In
Civil Engineering
(Structural Engineering)**



**Department of Civil Engineering
National Institute of Technology Rourkela
Odisha -769008, India
May 2012**

STUDY OF TORSIONAL BEHAVIOUR OF RECTANGULAR REINFORCED CONCRETE BEAMS WRAPPED WITH GFRP

*A thesis
Submitted by*

**Chhabirani Tudu
(210CE2277)**

*In partial fulfillment of the requirements
for the award of the degree of*

**Master of Technology
In
Civil Engineering
(Structural Engineering)**

**Under The Guidance of
Prof. Asha Patel**



**Department of Civil Engineering
National Institute of Technology Rourkela
Odisha -769008, India
May 2012**



DEPARTMENT OF CIVIL ENGINEERING
NATIONAL INSTITUTE OF TECHNOLOGY
ROURKELA, ODISHA-769008

CERTIFICATE

This is to certify that the thesis entitled, **“STUDY OF TORSIONAL BEHAVIOUR OF RECTANGULAR REINFORCED CONCRETE BEAMS WRAPPED WITH GFRP”** submitted by **CHHABIRANI TUDU** bearing Roll No. **210CE2277** in partial fulfilment of the requirements for the award of **Master of Technology** degree in **Civil Engineering** with specialization in **“Structural Engineering”** during 2010-2012 session at the National Institute of Technology, Rourkela is an authentic work carried out by her under my supervision and guidance.

To the best of my knowledge, the matter embodied in the thesis has not been submitted to any other University / Institute for the award of any Degree or Diploma.

Date: 25.05.2012

Place: Rourkela

Prof. Asha Patel

Department of Civil Engineering

National Institute of Technology

Rourkela, Odisha

ACKNOWLEDGEMENTS

First and foremost, praise and thanks goes to my God for the blessing that has bestowed upon me in all my endeavors.

I am deeply indebted to **Prof. Asha Patel**, Professor of Structural Engineering Division, my advisor and guide, for the motivation, guidance, tutelage and patience throughout the research work. I appreciate his broad range of expertise and attention to detail, as well as the constant encouragement he has given me over the years. There is no need to mention that a big part of this thesis is the result of joint work with him, without which the completion of the work would have been impossible.

I am grateful to **Prof. N Roy**, Head, Department of Civil Engineering for his valuable suggestions during the synopsis meeting and necessary facilities for the research work.

I extend my sincere thanks to **Mr. S. K. Sethi, Mr. R. Lugun, and Mr. Sushil** and the administrative staff of Structural Engineering Division for their timely help and encouragement for this work.

I would like to thank my parents and sisters. Without their love, patience and support, I could not have completed this work.

Finally, I wish to thank all my friends for the encouragement during these difficult years, especially, **Snehash, Haran, Snigdha, Bijily, Param, Hemanth, Soumya & Sukumar.**

Chhabirani Tudu

Roll No-210CE2277

Department of Civil Engineering

N.I.T Rourkela

ABSTRACT

Fiber Reinforced Polymer (FRP) as an external reinforcement is used extensively to deal with the strength requirements related to flexure and shear in structural systems. But the strengthening of members subjected to torsion is explored only recently. Torsion failure is an undesirable brittle form of failure which should be avoided specially in the earthquake prone areas. In the present work, the behaviour and performance of rectangular reinforced concrete beams strengthened with externally bonded Glass Fibre Reinforced Polymer (GFRP) fabrics subjected to combined flexure and torsion is studied experimentally.

Rectangular RC beams externally bonded with GFRP fabrics were tested to failure using an arrangement which transfer torque to the central part of the beam through two opposite cantilevers called moment arms. Each arm is subjected to equal static loading during the experiment. Total nine RC beams were cast and tested for the study. All the beams were designed to fail in torsion. One of the beam was used as a control beam and eight beams were strengthened using different configurations and different types of GFRP fabrics. The study is restricted to continuously wrapped GFRP fabrics.

Experimental data on ultimate & first cracking loads, angle of twist and failure modes of each of the beams were obtained. The effect of different types and configuration of GFRP on first crack load, ultimate load carrying capacity and failure mode of the beams were investigated.

The experimental results have been validated with finite element analysis by using ANSYS software and found to be in good agreement with analytical values. The experimental results show that externally bonded GFRP can increase the torsional capacity of the beam significantly. The results also indicate that the most effective configuration is the full-wrap of GFRP fabrics. In addition GFRP applied in 45^0 with axis of the beam gives more strength than GFRP applied in 90^0 with the axis of the beam.

TABLE OF CONTENTS

Title	Page No.
ACKNOWLEDGEMENTS	i
ABSTRACT	ii
TABLES OF CONTENTS	iii
LIST OF TABLES	vii
LIST OF FIGURES	viii
ABBREVIATIONS	xii
NOTATIONS	xiii
CHAPTER 1 INTRODUCTION	
1.1 Overview	1
1.2 Torsional strengthening of beams	3
1.3 Advantages and disadvantages of FRP	4
1.3.1 Advantages	4
1.3.2 Disadvantages	5
1.4 Organization of thesis	6
CHAPTER 2 REVIEW OF LITERATURE	
2.1 Brief review	7
2.2 Literature review on Torsional strengthening of RC beam	8
2.3 Critical observation from the literature	14
2.4 Objective and scope of the present work	14

CHAPTER 3 EXPERIMENTAL STUDY

3.1	Materials	15
3.1.1	Concrete	15
3.1.2	Cement	16
3.1.3	Fine Aggregate	16
3.1.4	Coarse Aggregate	17
3.1.5	Water	17
3.1.6	Fiber Reinforced Polymer (FRP)	17
3.1.7	Mix Design Of M20 Grade Concrete	19
3.1.8	Reinforcement	19
3.1.8.1	Detailing Of Reinforcement in R.C. Rectangular-Beams	20
3.2	Experimental study	21
3.3	Casting of specimen	21
3.3.1	Characteristics Strength of Specimens	22
3.3.2	Form Work	22
3.3.3	Mixing Of Concrete	23
3.3.4	Compaction	23
3.3.5	Curing Of Concrete	23
3.4	Fabrication of GFRP plate	24
3.5	Determination of ultimate stress, ultimate load and Young's modulus	26
3.6	Strengthening of beams	27
3.7	Experimental setup	29
3.7.1	Testing of Beams	31

3.7.1.1	Beam no.1 (Control Beam)	31
3.7.1.2	Beam No.2 (Beam fully wrapped with Unidirectional GFRP)	33
3.7.1.4	Beam No.3 (Beam fully wrapped with Bidirectional GFRP)	36
3.7.1.5	Beam No.4 (Beam wrapped with 10cm unidirectional GFRP -90 ⁰)	39
3.7.1.6	Beam No.5 (Beam wrapped with 10cm Bidirectional GFRP -90 ⁰)	41
3.7.1.7	Beam No.6 (Beam wrapped with 5cm Unidirectional GFRP -90 ⁰)	44
3.7.1.8	Beam No.7 (Beam wrapped with 5cm Bidirectional GFRP -90 ⁰)	46
3.7.1.9	Beam No.8 (Beam wrapped with 5cm Unidirectional GFRP -45 ⁰)	49
3.7.1.10	Beam No.9 Beam wrapped with 5cm Bidirectional GFRP-45 ⁰)	52
3.8	Summary	54

CHAPTER 4 NUMERICAL ANALYSIS USING ANSYS

4.1	Introduction	55
4.2	Finite element Modelling	55
4.2.1	Reinforced Concrete	55
4.2.2	Steel Reinforcement	56
4.2.3	Steel Plates	57
4.2.4	Laminates	57
4.3	Material Properties	58
4.4	Geometry and loading conditions	58

CHAPTER 5 RESULTS AND DISCUSSIONS

5.1	Experimental Results	62
5.2	Failure Modes	62
5.3	Torsional moment and angle of twist analysis	64
5.3.1	Torsional moment and Angle of twist Analysis of all Beams	64
5.3.2	Torsional moment and angle of twist analysis of beams wrapped with different series of wrapping	74
5.3.3	Torsional moment and angle of twist analysis of beams wrapped with unidirectional GFRP	77
5.3.4	Torsional moment and Angle of twist Analysis of Beams Wrapped with Bidirectional GFRP	78
5.3.5	Torsional moment and Angle of twist Analysis of All Beams	79
5.3.6	Load and angle of twist Analysis of Beams Wrapped with GFRP in Different Orientation	80
5.3.6.1	Beams Wrapped with Uni GFRP at 90^0 and 45^0 angle making with Beam	80
5.3.6.2	Beams Wrapped with Bi GFRP at 90^0 and 45^0 angle making with Beam	80
5.3.6.3	Load and angle of twist Analysis of Beams Wrapped with GFRP in Different Orientation Compared with ANSYS results	82
5.4	Ultimate load carrying capacity	84
5.4.1	Increase in load carrying capacity	85

CHAPTER 6 CONCLUSIONS

6.1	Conclusions	85
6.2	Scope of the future work	86

REFERENCES	87
-------------------	----

LIST OF TABLES

Title	Page No
Table 3.1 Properties of Materials	18
Table 3.2 Design Mix Proportions	19
Table 3.3 Characteristics Strength of Specimens	26
Table3.4 Size of the specimens for tensile test	26
Table 3.5 Result of the specimens	27
Table 3.6 Relation between angle of twist and Torsional moment (Control Beam)	33
Table 3.7 Relation between angle of twist and Torsional moment of Beam 2	35
Table 3.8 Relation between angle of twist and Torsional moment of Beam 3	38
Table 3.9 Relation between angle of twist and Torsional moment of Beam 4	40
Table 3.10 Relation between angle of twist and Torsional moment of Beam 5	43
Table 3.11 Relation between angle of twist and Torsional moment of Beam 6	45
Table 3.12 Relation between angle of twist and Torsional moment of Beam 7	47
Table 3.13 Relation between angle of twist and Torsional moment of Beam 8	51
Table 3.14 Relation between angle of twist and Torsional moment of Beam 9	54
Table 4.1 Material properties and elements used in the modelling	58

LIST OF FIGURES

Title	Page No
Fig. 3.1 Reinforcement Detailing of Beam	20
Fig. 3.2 Reinforcement Detailing of Beam at Sec-A-A	20
Fig. 3.3 Reinforcement Cage	22
Fig. 3.4 Steel Frame Used For Casting of Beams	23
Fig.3.5 Uni-GFRP & Bi-GFRP Specimens for testing	25
Fig.3.6 Experimental set up of INSTRON 1195	25
Fig.3.7 Uni-GFRP & Bi-GFRP Failure of specimens after tensile test	26
Fig. 3.8 Application of epoxy and hardener on the beam	28
Fig 3.9 Roller used for the removal of air bubble	29
Fig. 3.10 Shear force and bending moment diagram for two point loading	30
Fig. 3.11 Experimental Setup of the Control Beam No.1	31
Fig. 3.12 Control Beam after Cracking	32
Fig. 3.13 Crack Pattern on face -1	32
Fig. 3.14 Crack Pattern on face -2	32
Fig. 3.15 Experimental Setup of the Beam 2	33
Fig. 3.16 Face-1 of Beam 2 after testing	34
Fig. 3.17 Face-2 of Beam 2 after testing	34
Fig. 3.18 Crack developed under GFRP in Beam 2	34
Fig. 3.19 Magnified picture of the crack patterns in Beam 2	35
Fig. 3.20 Experimental Setup of the Beam 3	36
Fig. 3.21 Beam 3 after testing	36
Fig. 3.22 Crack Pattern Developed Under GFRP in Beam 3	37

Fig. 3.23	Close view of Crack Pattern Developed under GFRP Beam 3	37
Fig. 3.24	Experimental Setup of the Beam 4	39
Fig. 3.25	Crack pattern after test of Beam 4	39
Fig. 3.26	Close view of crack pattern	39
Fig. 3.27	Crack developed under GFRP in Beam 4	40
Fig. 3.28	Beam 5 after testing	41
Fig. 3.29	Crack appeared between GFRP strips in Beam 5	41
Fig. 3.30	Magnified picture of crack developed between GFRP strips in Beam 5	42
Fig. 3.31	Crack developed Under GFRP strips in Beam 5	42
Fig. 3.32	Experimental Setup of the Beam 6	44
Fig. 3.33	Rupture of GFRP during testing of beam in Beam 6	44
Fig. 3.34	Crack pattern between GFRP sheets after testing in Beam 6	45
Fig. 3.35	Experimental Setup of the Beam 7	46
Fig. 3.36	Crack appeared during testing in Beam 7	46
Fig. 3.37	Rupture of GFRP occurred during testing in Beam 7	47
Fig. 3.38	Crack pattern under GFRP in Beam 7	47
Fig. 3.39	Experimental Setup of the Beam 8	49
Fig. 3.40	Hairline Crack developed between GFRP strips in Beam 8	49
Fig. 3.41	Rupture of GFRP strips occurred during test in Beam 8	50
Fig. 3.42	Crack pattern under GFRP strips in Beam 8	50
Fig. 3.43	Experimental Setup of the Beam 9	52
Fig. 3.44	Debonding of GFRP sheet in Beam 9	52
Fig. 3.45	Debonding of GFRP sheet in Beam 9	53
Fig. 3.46	Crack pattern under GFRP sheets in Beam 9	53
Fig. 4.1	SOLID65 element	56

Fig. 4.2	BEAM188 element	56
Fig. 4.3	SOLID45 element	57
Fig. 4.4	SHELL91 element	58
Fig. 4.5	Reinforcement model in ANSYS	59
Fig. 4.6	Beam model in ANSYS with FRP making 450	60
Fig. 4.7	Beam model with FRP in ANSYS	60
Fig. 4.8	Deflected shape of Beam model in ANSYS	61
Fig. 5.1	Torsional Moment vs. Angle of Twist Curve for Control Beam-1	65
Fig. 5.2	Torsional Moment vs. Angle of Twist Curve for Beam-2	66
Fig. 5.3	Torsional Moment vs. Angle of Twist Curve for Beam-3	67
Fig. 5.4	Torsional Moment vs. Angle of Twist Curve for Beam-4	68
Fig. 5.5	Torsional Moment vs. Angle of Twist Curve for Beam-5	69
Fig. 5.6	Torsional Moment vs. Angle of Twist Curve for Beam-6	70
Fig. 5.7	Torsional Moment vs. Angle of Twist Curve for Beam-7	71
Fig. 5.8	Torsional Moment vs. Angle of Twist Curve for Beam-8	72
Fig. 5.9	Torsional Moment vs. Angle of Twist Curve for Beam-9	73
Fig. 5.10	Torsional Moment vs. Angle of Twist Curve for Beam-2 and Beam-3	74
Fig. 5.11	Torsional Moment vs. Angle of Twist Curve for Beam-4 and Beam-5	75
Fig. 5.12	Torsional Moment vs. Angle of Twist Curve for Beam-6 and Beam-7	75
Fig. 5.13	Torsional Moment vs. Angle of Twist Curve for Beam-8 and Beam-9	76
Fig. 5.14	Torsional Moment vs. Angle of Twist Curve for Beam-1, Beam-2, Beam-4, Beam-6 and Beam-8	77
Fig. 5.15	Torsional Moment vs. Angle of Twist Curve for Beam-1, Beam-3, Beam-5, Beam-7 and Beam-9	78
Fig. 5.16	Torsional Moment vs. Angle of Twist Curve for All Beams	79
Fig. 5.17	Torsional Moment vs. Angle of Twist Curve for Beam-6 and Beam-8	80

Fig. 5.18	Torsional Moment vs. Angle of Twist Curve Beam-7 and Beam-9	80
Fig. 5.19	Torsional Moment vs. Angle of Twist Curve for beams where GFRP applied in different orientations	81
Fig. 5.20	Torsional Moment vs. Angle of Twist Curve for beams where Uni-GFRP applied at 90° orientations	82
Fig. 5.21	Torsional Moment vs. Angle of Twist Curve for beams where Bi-GFRP applied at 90° orientations	82
Fig. 5.22	Torsional Moment vs. Angle of Twist Curve for beams where Uni-GFRP applied at 45° orientations	83
Fig. 5.23	Torsional Moment vs. Angle of Twist Curve for beams where Bi-GFRP applied at 45° orientations	83
Fig. 5.24	Ultimate Load carrying capacity	84
Fig. 5.25	Percentage increase in the Ultimate Carrying capacity w.r.t Control Beam 1	85

ABBREVIATIONS

ACI	American Concrete Institute
ANSYS	Analysis System
CFS	Carbon Fiber Sheet
FE	Finite Element
FRP	Fibre Reinforced Polymer
GFRP	Glass Fibre Reinforced Polymer
HYSD	High Yield Strength Deformed
IS	Indian Standard
PSC	Portland slag cement
RC	Reinforced Concrete
SMMT	Softened Membrane Model for Torsion
W/C	water-cementitious ratio

NOTATIONS

l	Length of cantilever part
l_{eff}	Effective length
D	Overall depth of the beam
B	Breadth of beam
L	Overall length of the beam
f_{ck}	Characteristic cube compressive strength of concrete
Φ	Diameter of reinforcement
f_y	Tensile strength of reinforcement bars

CHAPTER 1

INTRODUCTION

1.1. OVERVIEW

During its whole life span, nearly all engineering structures ranging from residential buildings, an industrial building to power stations and bridges faces degradation or deteriorations. The main causes for those deteriorations are environmental effects including corrosion of steel, gradual loss of strength with ageing, variation in temperature, freeze-thaw cycles, repeated high intensity loading, contact with chemicals and saline water and exposure to ultra-violet radiations. Addition to these environmental effects earthquakes is also a major cause of deterioration of any structure. This problem needs development of successful structural retrofit technologies. So it is very important to have a check upon the continuing performance of the civil engineering infrastructures. The structural retrofit problem has two options, repair/retrofit or demolition/reconstruction. Demolition or reconstruction means complete replacement of an existing structure may not be a cost-effective solution and it is likely to become an increasing financial burden if upgrading is a viable alternative. Therefore, repair and rehabilitation of bridges, buildings, and other civil engineering structures is very often chosen over reconstruction for the damage caused due to degradation, aging, lack of maintenance, and severe earthquakes and changes in the current design requirements.

Previously, the retrofitting of reinforced concrete structures, such as columns, beams and other structural elements, was done by removing and replacing the low quality or damaged concrete or/and steel reinforcements with new and stronger material. However, with the introduction of new advanced composite materials such as fiber reinforced polymer (FRP) composites, concrete members can now be easily and effectively strengthened using externally bonded FRP composites

Retrofitting of concrete structures with wrapping FRP sheets provide a more economical and technically superior alternative to the traditional techniques in many situations because it offers high strength, low weight, corrosion resistance, high fatigue resistance, easy and rapid installation and minimal change in structural geometry. In addition, FRP manufacturing offers a unique opportunity for the development of shapes and forms that would be difficult or impossible with the conventional steel materials. Although the fibers and resins used in FRP systems are relatively expensive compared with traditional strengthening materials, labour and equipment costs to install FRP systems are often lower. FRP systems can also be used in areas with limited access where traditional techniques would be impractical.

Several investigators took up concrete beams and columns retrofitted with carbon fiber reinforced polymer (CFRP) glass fiber reinforced polymer (GFRP) composites in order to study the enhancement of strength and ductility, durability, effect of confinement, preparation of design guidelines and experimental investigations of these members. The results obtained from different investigations regarding enhancement in basic parameters like strength/stiffness, ductility and durability of structural members retrofitted with externally bonded FRP composites, though quite encouraging, still suffers from many

limitations. This needs further study in order to arrive at recognizing FRP composites as a potential full proof structural additive. FRP repair is a simple way to increase both the strength and design life of a structure. Because of its high strength to weight ratio and resistance to corrosion, this repair method is ideal for deteriorated concrete structure.

1.2. TORSIONAL STRENGTHENING OF BEAMS

Early efforts for understanding the response of plain concrete subjected to pure torsion revealed that the material fails in tension rather than shear. Structural members curved in plan, members of a space frame, eccentrically loaded beams, curved box girders in bridges, spandrel beams in buildings, and spiral stair-cases are typical examples of the structural elements subjected to torsional moments and torsion cannot be neglected while designing such members. Structural members subjected to torsion are of different shapes such as T-shape, inverted L-shape, double T-shapes and box sections. These different configurations make the understanding of torsion in RC members a complex task.

In addition, torsion is usually associated with bending moments and shearing forces, and the interaction among these forces is important. Thus, the behaviour of concrete elements in torsion is primarily governed by the tensile response of the material, particularly its tensile cracking characteristics. Spandrel beams, located at the perimeter of buildings, carry loads from slabs, joists, and beams from one side of the member only. This loading mechanism generates torsional forces that are transferred from the spandrel beams to the columns. Reinforced concrete (RC) beams have been found to be deficient in torsional capacity and in need of strengthening. These deficiencies occur for several reasons, such as insufficient stirrups resulting from construction errors or inadequate design, reduction

in the effective steel area due to corrosion, or increased demand due to a change in occupancy.

Similar to the flexure and shear strengthening, the FRP fabric is bonded to the tension surface of the RC members for torsion strengthening. In the case of torsion, all sides of the member are subjected to diagonal tension and therefore the FRP sheets should be applied to all the faces of the member cross section. However, it is not always possible to provide external reinforcement for all the surfaces of the member cross section. In cases of inaccessible sides of the cross section, additional means of strengthening has to be provided to establish the adequate mechanism required to resist the torsion. The effectiveness of various wrapping configurations indicated that the fully wrapped beams performed better than using FRP in strips.

1.3. ADVANTAGES AND DISADVANTAGES OF FRP

1.3.1. Advantages

There have been several important advances in materials and techniques for structural rehabilitation, including a new class of structural materials such as fiber-reinforced polymers (FRP). One such technique for strengthening involves adding external reinforcement in the form of sheets made of FRP. Advanced materials offer the designer a new combination of properties not available from other materials and effective rehabilitation systems. Strengthening structural elements using FRP enables the designer to selectively increase their ductility, flexure, and shear capacity in response to the increasing seismic and service load demands. For columns, wrapping with FRP can significantly improve the strength and ductility.

A potent advantage of using FRP as an alternate external confinement to steel is the high strength to weight ratio comparisons. In order to achieve an equivalent confinement, FRP plates are up to 20% less dense than steel plates and are at least twice as strong, if not more. Manufacture of modern composites is, then, possible in reduced sections and allows composite plates to be shaped on-site. The lower density allows easier placement of confinement in application. Design of external confinement to a structure should be made with conservative adjustments to the primary structures dead weight load. Changes of the stiffness of members should be considered when redesigning the structure. The improved behaviour of FRP wrapped members reduces the strains of internal steel reinforcement thereby delaying attainment of yielding. Much like internal steel confinement in longitudinal and lateral axes, external confinement exerts a similar pressure on the concrete as well as to the internal steel. Furthermore, FRP have high corrosive resistance equating to material longevity whilst within aggressive environments. Such durability makes for potential savings in long-term maintenance costs.

1.3.2. Disadvantages

With the above advantages FRP does also have some disadvantages as follows: The main disadvantage of externally strengthening structures with fiber composite materials is the risk of fire, vandalism or accidental damage, unless the strengthening is protected. As FRP materials are lightweight they tend to poses aerodynamic instability. Retrofitting using fiber composites are more costly than traditional techniques. Experience of the long-term durability of fiber composites is not yet available. This may be a disadvantage for structures for which a very long design life is required but can be overcome by

appropriate monitoring. This technique need highly trained specialists. More over there is lack of standards and design guides.

1.4 ORGANIZATION OF THESIS

Chapter 1 gives a brief introduction to the use of GFRP as externally bonded reinforcement to strengthen the concrete members of buildings. This chapter also includes the advantages and disadvantages of FRP.

Chapter 2 reviews the literatures on prediction of torsional behaviour of RC beams wrapped with FRP have been discussed. The objectives and scope of the proposed research work are identified in this Chapter.

Chapter 3 discusses the details of experimental studies conducted and gives the test results of the beams which were tested under two-point loading arrangement.

Chapter 4 gives all the experimental results of all beams with different types of layering and orientation of GFRP. This chapter describes the failure modes, load-angle of twist analysis and ultimate load carrying capacity of the beams.

Finally, in Chapter 5, the summary and conclusions are given. Recommendations for improved methods for estimating torsional behaviour of RC beams are summarised. The scope for future work is also discussed.

CHAPTER 2

REVIEW OF LITERATURE

2.1 BRIEF REVIEW

Externally bonded, FRP sheets are currently being studied and applied around the world for the repair and strengthening of structural concrete members. Strengthening with Fiber Reinforced Polymers (FRP) composite materials in the form of external reinforcement is of great interest to the civil engineering community. FRP composite materials are of great interest to the civil engineering community because of their superior properties such as high stiffness and strength as well as ease of installation when compared to other repair materials. Also, the non-corrosive and nonmagnetic nature of the materials along with its resistance to chemicals made FRP an excellent option for external reinforcement.

Research on FRP material for use in concrete structures began in Europe in the mid 1950's by Rubinsky and Rubinsky, 1954 and Wines, J. C. et al., 1966. The pioneering work of bonded FRP system can be credited to Meier (Meier 1987); this work led to the first on-site repair by bonded FRP in Switzerland (Meier and Kaiser 1991). Japan developed its first FRP applications for repair of concrete chimneys in the early 1980s (ACI 440 1996). By 1997 more than 1500 concrete structures worldwide had been strengthened with externally bonded FRP materials. Thereafter, many FRP materials with different types of fibres have been developed. FRP products can take the form of bars, cables, 2-D and 3-D grids, sheet materials and laminates. With the increasing usage of new materials of FRP composites, many research works, on FRPs improvements of processing technology and other different aspects have been performed.

Though several researchers have been engaged in the investigation of the strengthened concrete structures with externally bonded FRP sheets/laminates/fabrics, no country yet has national design code on design guidelines for the concrete structures retrofitted using FRP composites. However, several national guidelines (The Concrete Society, UK: 2004; ACI 440:2002; FIB: 2001; ISIS Canada: 2001; JBDPA: 1999) offer the state of the art in selection of FRP systems and design and detailing of structures incorporating FRP reinforcement. On the contrary, there exists a divergence of opinion about certain aspects of the design and detailing guidelines. This is to be expected as the use of the relatively new material develops worldwide. Much research is being carried out at institutions around the world and it is expected that design criteria will continue to be enhanced as the results of this research become known in the coming years.

Several investigators like Saadatmanesh et al., (1994); Shahawy, (2000) took up FRP strengthened circular or rectangular columns studying enhancement of strength and ductility, durability, effect of confinement, preparation of design guidelines and experimental investigations of these columns.

Saadatmanesh et al. (1994) studied the strength and ductility of concrete columns externally reinforced with fibre composite strap. Chaallal and Shahawy (2000) reported the experimental investigation of fiber reinforced polymer-wrapped reinforced concrete column under combined axial-flexural loading. Obaidat et al (2010) studied the Retrofitting of reinforced concrete beams using composite laminates and the main variables considered are the internal reinforcement ratio, position of retrofitting and the length of CFRP.

2.2 LITERATURE REVIEW ON TORSIONAL STRENGTHENING OF RC BEAM

Most of the research projects investigating the use of FRP focused on enhancing the flexural and shear behaviour, ductility, and confinement of concrete structural members. A

limited number of mostly experimental studies were conducted to investigate torsion strengthening of RC members.

Ghobarah et al. (2002) conducted an experimental investigation on the improvement of the torsional resistance of reinforced concrete beams using fiber-reinforced polymer (FRP) fabric. A total of 11 beams were tested. Three beams were designated as control specimens and eight beams were strengthened by FRP wrapping of different configuration and then tested. Both glass and carbon fibers were used in the torsional resistance upgrade. Different wrapping designs were evaluated. The reinforced concrete beams were subjected to pure torsional moments. The load, twist angle of the beam, and strains were recorded. Improving the torsional resistance of reinforced concrete beams using FRP was demonstrated to be viable. The effectiveness of various wrapping configurations indicated that the fully wrapped beams performed better than using strips. The 45° orientation of the fibers ensures that the material is efficiently utilized

Panchacharam and Belarbi (2002) experimentally found out that externally bonded GFRP sheets can significantly increase both the cracking and the ultimate torsional capacity. The behaviour and performance of reinforced concrete member strengthened with externally bonded Glass FRP (GFRP) sheets subjected to pure torsion was presented. The variables considered in the experimental study include the fiber orientation, the number of beam faces strengthened (three or four), the effect of number of FRP plies used, and the influence of anchors in U-wrapped test beams. Experimental results reveal that externally bonded GFRP sheets can significantly increase both the cracking and the ultimate torsional capacity. Predicted strengths of the test beams using the proposed theoretical models were found to be in good agreement with the experimental results.

Salom et al. (2004) conducted both experimental and analytical programs focused on the torsional strengthening of reinforced concrete spandrel beams using composite laminates.

The variables considered in this study included fiber orientation, composite laminate, and effects of a laminate anchoring system. Current torsional strengthening and repair methods are time and resource intensive, and quite often very intrusive. The proposed method however, uses composite laminates to increase the torsional capacity of concrete beams.

Jing et al. (2005) made an experimental investigation on the response of reinforced concrete box beam under combined actions of bending moment, shear and cyclic torque, strengthened with externally bonded carbon fiber reinforced polymer sheets. Three strengthened box beams and one reference box beam were tested. The main parameters of this experiment were the amount of CFS and the wrapping schemes. The failure shapes, torsional capacities, deformation capacities, rigidity attenuations and hysteresis behaviours of specimens were studied in detail. The experimental results indicated that the contribution of externally bonded CFS to the aseismic capacity of box beam is significant. Based on the test results and analysis, restoring force model of CFS strengthened R.C. box beam under combined actions of bending moment, shear and cyclic torque was established.

Al-Mahaidi and Hii (2006) focuses on the bond-behaviour of externally bonded CFRP in an overall investigation of torsional strengthening of solid and box-section reinforced concrete beams. Significant levels of debonding prior to failure by CFRP rupture were measured in experiments with photogrammetry. Numerical work was carried out using non-linear finite element (FE) modelling. Good agreement in terms of torque-twist behaviour, steel and CFRP reinforcement responses, and crack patterns was achieved. The addition of a bond-slip model between the CFRP reinforcement and concrete meant that the debonding mechanisms prior to and unique failure modes of all the specimens were modelled correctly as well. Numerical work was carried out using non-linear finite element (FE) modelling. Good agreement in terms of torque-twist behaviour, steel and CFRP reinforcement responses, and crack patterns was achieved.

Very few analytical models are available for predicting the section capacity (Ameli and Ronagh 2007; Hii and Al-Mahadi 2006; Rahal and Collins 1995).

Santhakumar et al. (2007) presented the numerical study on unretrofitted and retrofitted reinforced concrete beams subjected to combined bending and torsion. Different ratios between twisting moment and bending moment are considered. The finite elements adopted by ANSYS are used for this study. For the purpose of validation of the finite element model developed, the numerical study is first carried out on the un-retrofitted reinforced concrete beams that were experimentally tested and reported in the literature. Then the study has been extended for the same reinforced concrete beams retrofitted with carbon fiber reinforced plastic composites with $\pm 45^\circ$ and $0/90^\circ$ fiber orientations. The present study reveals that the CFRP composites with $\pm 45^\circ$ fiber orientations are more effective in retrofitting the RC beams subjected to combined bending and torsion for higher torque to moment ratios.

Ameli et al. (2007) experimentally investigated together with a numerical study on reinforced concrete beams subjected to torsion that are strengthened with FRP wraps in a variety of configurations. Experimental results show that FRP wraps can increase the ultimate torque of fully wrapped beams considerably in addition to enhancing the ductility.

Chalioris (2007) addressed an analytical method for the prediction of the entire torsional behaviour of reinforced concrete (RC) beams strengthened with externally bonded fibre-reinforced-polymers (FRP) materials. The proposed approach combines two different theoretical models; a smeared crack analysis for plain concrete in torsion for the prediction of the elastic behaviour and the cracking torsional moment, and a properly modified softened truss theory for the description of the post-cracking torsional response and the calculation of the ultimate torque capacity. The contribution of the FRPs is implemented by specially developed (a) equations in a well-known truss model and (b) stress - strain relationships of

softened and FRP-confined concrete. In order to check the accuracy of the proposed methodology an experimental program of 12 rectangular beams under torsion was conducted. Tested beams were retrofitted using epoxy-bonded Carbon FRP continuous sheets and discrete strips as external reinforcement. Strengthened beams with continuous sheets performed improved torsional behaviour and higher capacity than the beams with strips, since failure occurred due to fibre rupture. Comparisons between analytically predicted results and experimental ones indicated that the proposed behavioural model provides rational torque curves and calculates the torsional moments at cracking and at ultimate with satisfactory accuracy.

Hii and Al-Mahaidi (2007) briefly recounted the experimental work in an overall investigation of torsional strengthening of solid and box-section reinforced concrete beams with externally bonded carbon fiber-reinforced polymer (CFRP).

Mohammadizadeh et al. (2008) found that the increase in CFRP contribution to torsional strength concerning the beams strengthened by one ply and two plies of CFRP sheets is close for various steel reinforcement ratios, when compared to increasing the total amount of steel reinforcement.

Behera et al. (2008) conducted an experimental programme consisting of casting and testing of beams with “U” wrap was conducted in the laboratory to study the effect of aspect ratio (ratio of depth to breadth), constituent materials of ferrocement (viz., number of mesh layers, yield strength of mesh layers and compressive strength of mortar) and concrete strength on ultimate torsional strength and twist. This experimental results briefly recounts that wrapping on three sides enhance the ultimate torque and twist.

Deifalla and Ghobarah (2010) developed an analytical model for the case of the RC beams strengthened in torsion. The model is based on the basics of the modified compression field

theory, the hollow tube analogy, and the compatibility at the corner of the cross section. Several modifications were implemented to be able to take into account the effect of various parameters including various strengthening schemes where the FRP is not bonded to all beam faces, FRP contribution, and different failure modes. The model showed good agreement with the experimental results. The model predicted the strength more accurately than a previous model. The model predicted the FRP strain and the failure mode.

Mahmood and Mahmood (2011) conducted several experiments to study the torsional behaviour of prestressed concrete beams strengthened with CFRP sheets. They have taken eight medium-scale reinforced concrete beams (150mmx250mm) cross section and 2500mm long were constructed pure torsion test. All beams have four strands have no eccentricity (concentric) at neutral axis of section. There are classified into two group according uses of ordinary reinforcements. Where four beams with steel reinforcements, for representing partial prestressing beams, while other four beams have not steel reinforcements for representing full prestressing beams. The applied CFRP configurations are full wrap, U jacked, and stirrups with spacing equal to half the depth of beam along its entire length. The test results have shown that the performance of fully wrapped prestressed beams is superior to those with other form of sheet wrapping. All the strengthened beams have shown a significant increase in the torsional strength compared with the reference beams. Also, this study included the nonlinear finite element analysis of the tested beams to predict a model for analyzing prestressed beams strengthening with CFRP sheets.

Zojaji and Kabir (2011) developed a new computational procedure to predict the full torsional response of reinforced concrete beams strengthened with Fiber Reinforced Plastics (FRPs), based on the Softened Membrane Model for Torsion (SMMT). To validate the proposed analytical model, torque-twist curves obtained from the theoretical approaches are compared with experimental ones for both solid and hollow rectangular sections

2.3 CRITICAL OBSERVATION FROM THE LITERATURE

From the above literature review it is clear that, none of these models predicted the full behaviour of RC beams wrapped with FRP, account for the fact that the FRP is not bonded to all beam faces, predicted the failure mode, or predicted the effective FRP strain using equations developed based on testing FRP strengthened beams in torsion. The reason is the complexity of the torsion problem and the lack of adequate experimental results required to understand the full behaviour.

2.4 OBJECTIVE AND SCOPE OF THE PRESENT WORK

The aim of present work is to study behaviour and performance of RCC rectangular beams strengthened with externally bonded Glass Fiber reinforced Polymer subjected to combined flexure and torsion. In the present work the behaviour of rectangular reinforced concrete beams, strengthened with GFRP is observed to know the practical feasibility of its application in the construction industry. Nine numbers of rectangular reinforced concrete beams are cast. All these beams except one beam are bonded with GFRP fabrics using epoxy in different size and orientations. These beams are subjected to torsion by applying gradually increasing static loading at the two cantilever moment arm of the beam to evaluate the increase in the torsional strength due to retrofitting. And the results are validated analytically by using finite element software ANSYS.

The variables considered in the experimental studies include

- (1) Fiber orientation (45° , 90° oriented uni-directional & bi-directional glass fiber fabrics)
- (2) GFRP configuration (continuously fully wrapped and wrapped in strips)
- (3) Fiber type (Unidirectional and Bi-directional GFRP woven fabrics)

The experimental results will be compared with the analytical results.

CHAPTER 3

EXPERIMENTAL STUDY

3.1 MATERIALS

3.1.1 Concrete

Concrete is a composite construction material composed of aggregate, cement and water. There are many formulations that have varied properties. The aggregate is generally coarse gravel or crushed rocks such as limestone, or granite, along with a fine aggregate such as sand. The cement, commonly Portland cement, and other cementitious materials such as fly ash and slag cement, serve as a binder for the aggregate. Various chemical admixtures are also added to achieve varied properties. Water is then mixed with this dry composite which enables it to be shaped (typically poured) and then solidified and hardened into rock-hard strength through a chemical process known as hydration. The water reacts with the cement which bonds the other components together, eventually creating a robust stone-like material. Concrete has relatively high compressive strength, but much lower tensile strength. The ultimate strength of concrete is influenced by the water-cementitious ratio (w/cm), the design constituents, and the mixing, placement and curing methods employed. All things being equal, concrete with a lower water-cement (cementitious) ratio makes a stronger concrete than that with a higher ratio. The quality of the paste formed by the cement and water largely determines the character of the concrete. Proportioning of the ingredients of concrete is

referred to as designing the mixture, and for most structural work the concrete is designed to give compressive strengths of 15 to 35 MPa.

3.1.2 Cement

Cement is a material, generally in powder form, that can be made into a paste usually by the addition of water and, when moulded or poured, will set into a solid mass. Numerous organic compounds used for adhering, or fastening materials, are called cements, but these are classified as adhesives, and the term cement alone means a construction material. The most widely used of the construction cements is Portland cement. It is a bluish-gray powder obtained by finely grinding the clinker made by strongly heating an intimate mixture of calcareous and argillaceous minerals. The chief raw material is a mixture of high-calcium limestone, known as cement rock, and clay or shale. Blast-furnace slag may also be used in some cements and the cement is called Portland slag cement (PSC). The colour of the cement is due chiefly to iron oxide. In the absence of impurities, the colour would be white, but neither the colour nor the specific gravity is a test of quality.

3.1.3 Fine Aggregate

Fine aggregate is natural sand which has been washed and sieved to remove particles larger than 5 mm and coarse aggregate is gravel which has been crushed, washed and sieved so that the particles vary from 5 up to 50 mm in size. The fine and coarse aggregate are delivered separately. Because they have to be sieved, a prepared mixture of fine and coarse aggregate is more expensive than natural all-in aggregate. Sand is used for making mortar and concrete and for polishing and sandblasting. Sands containing a

little clay are used for making moulds in foundries. Clear sands are employed for filtering water. Sand is sold by the cubic yard (0.76 m³) or ton (0.91 metric ton) but is always shipped by weight. The weight varies from 1,538 to 1,842 kg/m³, depending on the composition and size of grain. The fine aggregate is passing through 4.75 mm sieve and had a specific gravity of 2.67.

3.1.4 Coarse Aggregate

Coarse aggregate are the crushed stone is used for making concrete. The commercial stone is quarried, crushed, and graded. Much of the crushed stone used is granite, limestone, and trap rock.. The sizes are from 0.25 to 2.5 in (0.64 to 6.35 cm), although larger sizes may be used for massive concrete aggregate. Machine chorused granite broken stone angular in shape is use as coarse aggregate.

3.1.5 Water

In general water that is fit for drinking is considered fit for making concrete. Water should be free from acids, oils, alkalis, vegetables or other organic impurities. Soft water also produces weaker concrete. Water has mainly two functions in concrete mix. Firstly, it causes a chemical reaction with the cement to form cement paste in which the inert aggregate are held in suspension until the cement paste has hardened. And secondly it acts as a lubricant in the mixture of fine aggregate and cement.

3.1.6 Fiber Reinforced Polymer (FRP)

Fiber reinforced polymer (FRP) is a composite material made by combining two or more materials to give a new combination of properties. However, FRP is different from other composites in that its constituent materials are different at the molecular level and are mechanically separable. The mechanical and physical properties of FRP are controlled by its constituent properties and by structural configurations at micro level. Therefore, the

design and analysis of any FRP structural member requires a good knowledge of the material properties, which are dependent on the manufacturing process and the properties of constituent materials. FRP composite is a two phased material, hence its anisotropic properties. It is composed of fiber and matrix, which are bonded at interface. Each of these different phases has to perform its required function based on mechanical properties, so that the composite system performs satisfactorily as a whole. In this case, the reinforcing fiber provides FRP composite with strength and stiffness, while the matrix gives rigidity and environmental protection. A great majority of materials are stronger and stiffer in fibrous form than as bulk materials. A high fiber aspect ratio (length: diameter ratio) permits very effective transfer of load via matrix materials to the fibers, thus taking advantage of their excellent properties. Therefore, fibers are very effective and attractive reinforcement materials. They are widely used for strengthening of civil structures. There are many advantages of using FRPs: lightweight, good mechanical properties, corrosion-resistant, etc. Composites for structural strengthening are available in several geometries from laminates used for strengthening of members with regular surface to bidirectional fabrics easily adaptable to the shape of the member to be strengthened.

Table 3.1: Properties of materials

Materials	Specific Gravity
Cement	2.98
Fine Aggregate	2.5
Coarse Aggregate	2.78

3.1.7 Mix Design Of M20 Grade Concrete

1. Design Stipulations

- a) Characteristics strength (f_{ck}) = 20N/mm²
- b) Maximum water cement ratio (w/c) = 0.5
- c) Workability = 58 mm slump value

2. Materials Supplied

- a) Cement: Konark Portland Slag Cement
- b) Course aggregate: 20mm & 10 mm down
- c) Fine aggregate: Sand conforming to grading zone III

Trough trial method the mix proportion for M20 grade is as follows:

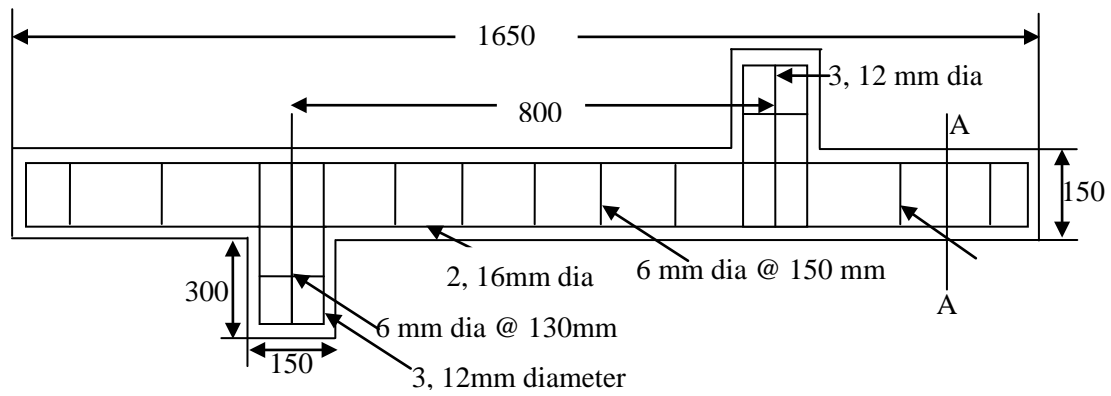
Table 3.2: Design Mix Proportions

Description	Cement	Sand (Fine Aggregate)	Course Aggregate	Water
Mix proportion (by weight)	1	1.8	3.6	0.5
Quantities of materials (in Kg/m ³) for each beam	46	84	168	26

3.1.8 Reinforcement

High-Yield Strength Deformed bars of 16 mm diameter, 12 mm diameter, 10 mm diameter are used for the longitudinal reinforcement and 6 mm diameter high-yield strength deformed bars are used as stirrups. The yield strength of steel reinforcements used in this experimental program is determined by performing the standard tensile test on the three specimens of each bar. The average tensile strength (f_y) of bars of 16mm ϕ bars is 494 N/mm², 12mm ϕ bars is 578N/mm², 10mm ϕ bars is 429 N/mm², 8mm ϕ bars is 523 N/mm² and of 6mm ϕ bars is 250N/mm².

3.1.8.1 Reinforcement Detailing Of The Beams



Top view of Torsional Beam

Fig: 3.1 Reinforcement Detailing of Beam

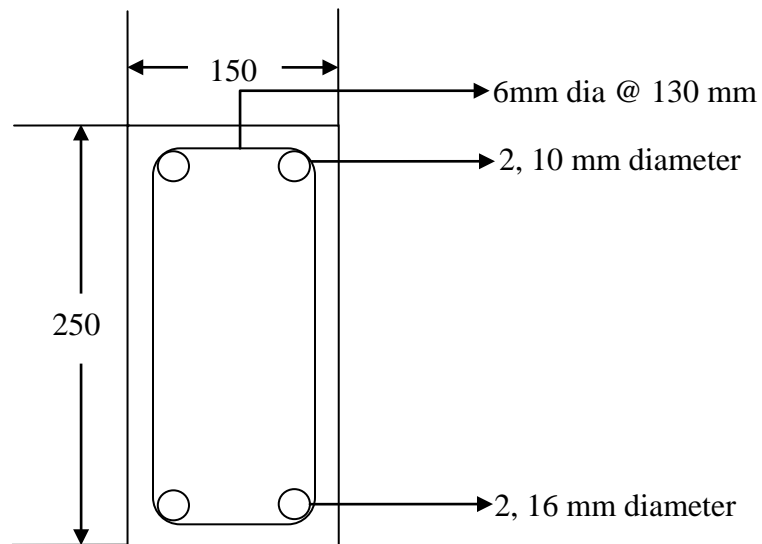


Fig: 3.2 Reinforcement Detailing of Beam at Sec-A-A

3.2 EXPERIMENTAL STUDY

Total nine numbers of reinforced concrete rectangular beams were cast for the experimental study. All the nine beams weak in torsion are cast, out of which one is taken as controlled beam and other eight beams are strengthened using glass fiber reinforced polymer (GFRP). The eight beams were strengthened with GFRP in four different series. In SERIES-1 two beams were continuously fully wrapped, one with unidirectional GFRP and other with bidirectional GFRP. In SERIES-2 two beams were wrapped with 10cm GFRP strips, one with unidirectional GFRP and other with bidirectional GFRP. In SERIES-3 two beams were wrapped with 5cm GFRP strips, one with unidirectional GFRP and other with bidirectional GFRP. In SERIES-4 two beams were wrapped with 5cm GFRP strips, one with unidirectional GFRP and other with bidirectional GFRP making 45^0 with the axis of the beam.

3.3 CASTING OF SPECIMEN

For conducting experiment, nine reinforced concrete Torsion beam specimen of size as Shown in the fig (Length of main beam (L) = 1.65m, Effective length (l_{eff}) = 1.6m. Breadth of main beam(B) = 0.15m, Depth of main beam(D) = 0.25m, Length of cantilever part (l) = 0.3m, Width of cantilever part= 0.15m, Depth of cantilever part= 0.25m, Distance of cantilever part from end of the beam= 0.35m) and all having the same reinforcement detailing are cast. The mix proportion is 0.5: 1:1.8:3.6 for water, cement, fine aggregate and course aggregate is taken. The mixing is done by using concrete mixture. The beams were cured for 28 days. For each beam three cubes, two cylinders and two prisms were casted to determine the compressive strength of concrete for 28 days.

3.3.1 Characteristics Strength of Specimens

Table 3.3: The characteristics of the specimens

Specimen	Configurations	No of Layers	Concrete cube compressive strength (N/mm ²)	Flexural Strength Of Concrete Prism (N/mm ²)	Split Tensile Strength of Concrete Cylinder (N/mm ²)
Beam No 1	Control beam	None	27.11	6	2.96
Beam No 2	Uni-GFRP Continuous fully wrap	2	31	5.83	2.68
Beam No 3	Bi-GFRP Continuous fully wrap	2	29.34	6.3	3.15
Beam No 4	10cm Uni-GFRP strips wrap	2	30.25	5.65	3.34
Beam No 5	10cm Bi-GFRP strips wrap	2	28.53	6	2.76
Beam No 6	5cm Uni-GFRP strips wrap	2	25.78	5.7	2.87
Beam No 7	5cm Bi-GFRP strips wrap	2	27.36	5.87	2.4
Beam No 8	5cm Uni-GFRP strips wrap(45 ⁰)	2	30	6.1	2.76
Beam No 9	5cm Bi-GFRP strips wrap(45 ⁰)	2	31.5	6.54	3.32

3.3.2 Form Work



Fig:3.3 Reinforcement Cage



Fig. 3.4 Steel Frame Used For Casting of Beams

3.3.3 Mixing Of Concrete

Mixing of concrete is done thoroughly with the help of machine mixer so that a uniform quality of concrete was obtained.

3.3.4 Compaction

Compaction is done with the help of needle vibrator in all the specimens .And care is taken to avoid displacement of the reinforcement cage inside the form work. Then the surface of the concrete is levelled and smoothened by metal trowel and wooden float

3.3.5 Curing Of Concrete

Curing is done to prevent the loss of water which is essential for the process of hydration and hence for hardening. It also prevents the exposure of concrete to a hot atmosphere and to drying winds which may lead to quick drying out of moisture in the concrete and there by subject it to contraction stresses at a stage when the concrete would not be strong

enough to resist them. Here curing is to be done by spraying water on the jute bags spread over the surface for a period of 7 days.

3.4 FABRICATION OF GFRP PLATE

There are two basic processes for moulding: hand lay-up and spray-up. The hand lay-up process is the oldest and simplest fabrication method. The process is most common in FRP marine construction. In hand lay-up process, liquid resin is placed along with FRP against finished surface. Chemical reaction of the resin hardens the material to a strong light weight product. The resin serves as the matrix for glass fibre as concrete acts for the steel reinforcing rods.

The following constituent materials were used for fabricating plates:

1. Glass Fibre
2. Epoxy as resin
3. Hardener as diamine (catalyst)
4. Polyvinyl alcohol as a releasing agent

A plastic sheet was kept on the plywood platform and a thin film of polyvinyl alcohol was applied as a releasing agent by the use of spray gun. Laminating starts with the application of a gel coat (epoxy and hardener) deposited in the mould by brush, whose main purpose was to provide a smooth external surface and to protect fibres from direct exposure from the environment. Steel roller was applied to remove the air bubbles. Layers of reinforcement were applied and gel coat was applied by brush. Process of hand lay-up is the continuation of the above process before gel coat is hardened. Again a plastic sheet was applied by applying polyvinyl alcohol inside the sheet as releasing agent. Then a heavy flat metal rigid platform was kept top of the plate for compressing

purpose. The plates were left for minimum 48 hours before transported and cut to exact shape for testing.

Plates were casted using two different glass fibres Uni-GFRP and Bi-GFRP of 2 layers which are loosely spaced and are tested.



Fig.3.5 Uni-GFRP & Bi-GFRP Specimens for testing



Fig.3.6 Experimental set up of INSTRON 1195

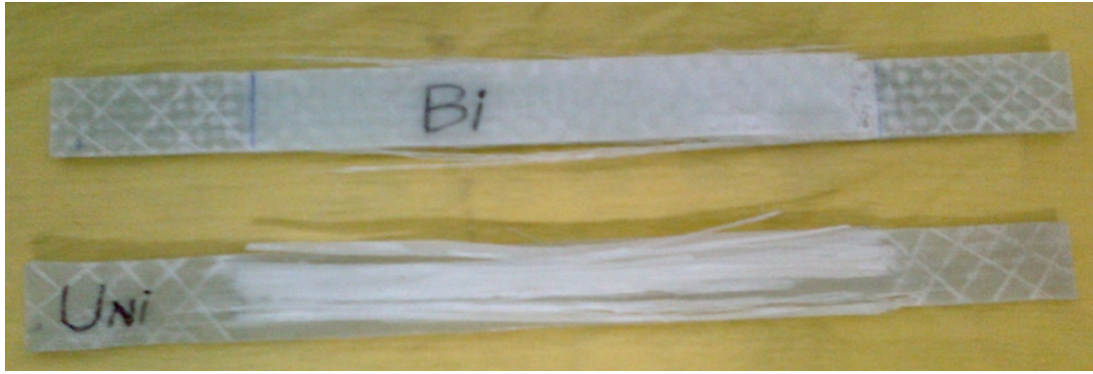


Fig.3.7 Failure of Uni-GFRP & Bi-GFRP Specimens after tensile test

Table3.4 Size of the specimens for tensile test

No. of layers	Length (cm)	Width (cm)	Thickness (cm)
2(Uni-GFRP)	15	2.3	0.15
2(Bi-GFRP)	15	2.3	0.3

3.5 DETERMINATION OF ULTIMATE STRESS, ULTIMATE LOAD AND YOUNGS MODULUS

The ultimate stress, ultimate load and young's modulus was determined experimentally by performing unidirectional tensile test on the specimens cut in longitudinal and transverse direction. The dimensions of the specimens are shown in Table 3.4. The specimens were cut from the plates by diamond cutter or by hex saw. After cutting by hex saw, it was polished in the polishing machine.

For measuring the young's modulus, the specimen is loaded in INSTRON 1195 universal tensile test machine to failure with a recommended rate of extension. Specimens were gripped in the upper jaw first and then gripped in the movable lower jaw. Gripping of the specimen should be proper to prevent slippage. Here, it is taken as 50 mm from each side.

Initially, the strain is kept zero. The load as well as extension was recorded digitally with the help of the load cell and an extensometer respectively. From these data, stress versus strain graph was plotted, the initial slope of which gives the Young's modulus. The ultimate stress and the ultimate load were obtained at the failure of the specimen. The average value of each of the specimens is given in the Table 3.3.

Table 3.5 Result of the specimens

No. of layers of the specimen	Ultimate stress (MPa)	Ultimate Load (KN)	Young's modulus(MPa)
2 Layers(Uni-GFRP)	338.2	23.33	8189
2 Layers(Bi-GFRP)	268.6	30.89	6158

3.6 STRENGTHENING OF BEAMS

At the time of bonding of fiber, the concrete surface is made rough using a coarse sand paper texture and then cleaned with an air blower to remove all dirt and debris. After that the epoxy resin is mixed in accordance with manufacturer's instructions. The mixing is carried out in a plastic container (100 parts by weight of Araldite LY 556 to 10 parts by weight of Hardener HY 951). After their uniform mixing, the fabrics are cut according to the size then the epoxy resin is applied to the concrete surface. Then the GFRP sheet is placed on top of epoxy resin coating and the resin is squeezed through the roving of the fabric with the roller. Air bubbles entrapped at the epoxy/concrete or epoxy/fabric interface are eliminated. During hardening of the epoxy, a constant uniform pressure is applied on the composite fabric surface in order to extrude the excess epoxy resin and to ensure good contact between the epoxy, the concrete and the fabric. This operation is

carried out at room temperature. Concrete beams strengthened with glass fiber fabric are cured for 24 hours at room temperature before testing.



Fig. 3.8 Application of epoxy and hardener on the beam



Fig 3.9 Roller used for the removal of air bubble

3.7 EXPERIMENTAL SETUP

The beams were tested in the loading frame of “Structural Engineering” Laboratory of National Institute of Technology, Rourkela. The testing procedure for the all the specimen is same. First the beams are cured for a period of 28 days then its surface is cleaned with the help of sand paper for clear visibility of cracks. The two-point loading arrangement was used for testing of beams. This has the advantage of a substantial region of nearly uniform moment coupled with very small shears, enabling the bending capacity of the central portion to be assessed. Two-point loading is conveniently provided by the arrangement shown in Figure. The load is transmitted through a load cell and spherical seating on to a spreader beam. The spreader beam is installed on rollers seated on steel

plates bedded on the test member with cement in order to provide a smooth levelled surface. The test member is supported on roller bearings acting on similar spreader plates. The specimen is placed over the two steel rollers bearing leaving 50 mm from the ends of the beam. The load is transmitted through a load cell via the square plates kept over the flange of the beam at a distance 105mm from the end. Loading was done by Hydraulic Jack of capacity 100 Tones.

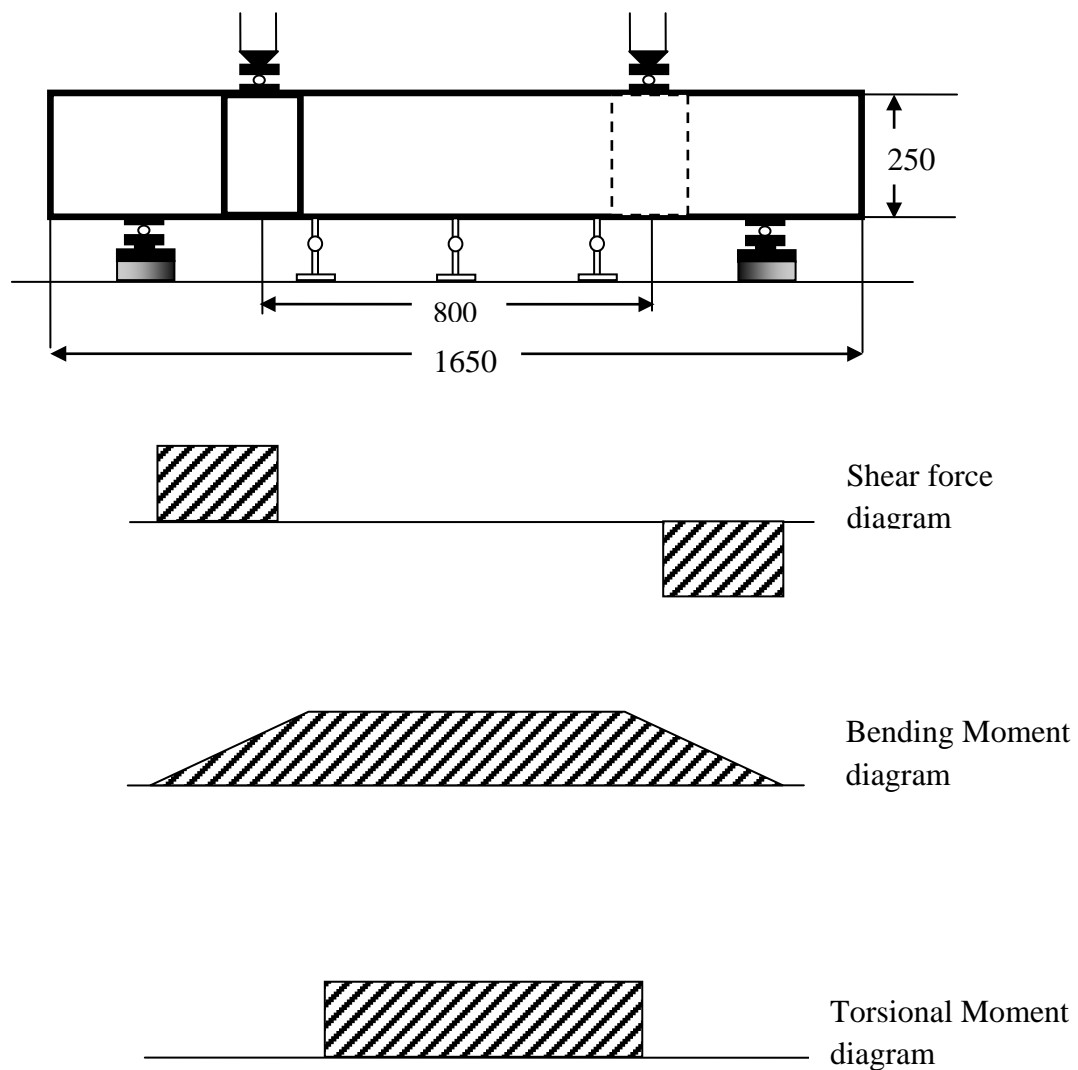


Fig. 3.10 Shear force and bending moment diagram for two point loading

3.7.1 Testing of Beams

All The nine beams were tested one by one. Eight with FRP and one without FRP which is taken as the control Beam .All of them are tested in the above arrangement. The gradual increase in load and the deformation in the strain gauge reading are taken throughout the test. The dial gauge reading shows the deformation. The load at which the first visible crack is developed is recorded as cracking load. Then the load is applied till the ultimate failure of the beam. The deflections at two salient points mentioned for the beams with and without GFRP are recorded with respect to increase of load and angle of twist is been calculated and are furnished in table. The data furnished in this chapter have been interpreted and discussed in the next chapter to obtain a conclusion.

3.7.1.1 BEAM NO.1

Control Beam



Fig. 3.11 Experimental Setup of the Control Beam No.1



Fig. 3.12 Control Beam after Cracking



Fig. 3.13 Crack Pattern on face -1



Fig. 3.14 Crack Pattern on face -2

Table 3.6 Relation between angle of twist and Torsional moment (Control Beam)

Torsional moment(KNm)	Angle of twist(rad/m) (Section-1)	Angle of twist(rad/m) (Section-2)	Remarks
0	0	0	
5.4	0.001	0.002	
8.1	0.002	0.003	
10.8	0.003	0.004	
13.5	0.004	0.005	
16.2	0.005	0.006	
18.9	0.006	0.008	
21.6	0.007	0.010	First hairline crack appeared(80KN)
24.3	0.009	0.012	
27	0.010	0.015	
29.7	0.012	0.017	
32.4	0.015	0.019	
35.1			Ultimate load(130KN)

3.7.1.2 BEAM NO.2

Beam fully wrapped with Unidirectional GFRP



Fig. 3.15 Experimental Setup of the Beam 2



Fig. 3.16 Face-1 of Beam 2 after testing



Fig. 3.17 Face-2 of Beam 2 after testing



Fig. 3.18 Crack developed under GFRP in Beam 2



Fig. 3.19 Magnified picture of the crack patterns in Beam 2

Table 3.7 Relation between angle of twist and Torsional moment of Beam 2

Torsional Moment(KNm)	Angle of twist(rad/m) (section-1)	Angle of twist (rad/m) (section-2)	Remarks
0	0	0	
2.7	0.000615	0.00099	
5.4	0.000692	0.00107	
8.1	0.000769	0.00115	
16.2	0.001	0.0017	
18.9	0.001	0.00191	
24.3	0.0012	0.00223	First cracking sound heard(100KN)
29	0.00184	0.00256	
35.1	0.0023	0.00346	
40.5	0.00261	0.00438	
43.2	0.00276	0.00523	
45.9	0.00292	0.0063	
48.6	0.00361	0.00699	
51.3	0.00446	0.00776	
54	0.00507	0.0083	
56.7	0.006	0.00884	
66.15			Ultimate load(245KN)

3.7.1.4 BEAM NO.3

Beam fully wrapped with Bidirectional GFRP



Fig. 3.20 Experimental Setup of the Beam 3



Fig. 3.21 Beam 3 after testing



Fig. 3.22 Crack Pattern Developed Under GFRP in Beam 3



Fig. 3.23 Close view of Crack Pattern Developed under GFRP Beam 3

Table 3.8 Relation between angle of twist and Torsional moment of Beam 3

Torsional Moment(KNm)	Angle of twist(rad/m) (section-1)	Angle of twist(rad/m) (section-2)	Remarks
0	0	0	
2.7	0.002	0.00353	
5.4	0.003	0.003769	
8.1	0.0038	0.0043	
16.2	0.00467	0.00584	
18.9	0.00543	0.00646	
24.3	0.00623	0.00707	
29	0.0064	0.00787	
35.1	0.00692	0.00829	First cracking sound heard(140KN)
40.5	0.0071	0.0089	
43.2	0.00719	0.00915	
45.9	0.00725	0.00945	
48.6	0.00736	0.0098	
51.3	0.008	0.01	
54	0.00846	0.011	
56.7			Ultimate load(210KN)

3.7.1.5 BEAM NO.4

Beam wrapped with 10cm unidirectional GFRP (90°)



Fig. 3.24 Experimental Setup of the Beam 4



Fig. 3.25 Crack pattern after test of Beam 4 Fig. 3.26 Close view of crack pattern



Fig. 3.27 Crack developed under GFRP in Beam 4

Table 3.9 Relation between angle of twist and Torsional moment of Beam 4

Torsional moment (KNm)	Angle of twist (rad/m) (section-1)	Angle of twist (rad/m) (section-2)	Remarks
0	0	0	
2.7	0.000923	0.00338	
5.4	0.00123	0.00392	
8.1	0.00138	0.00415	
10.8	0.00153	0.00538	
13.5	0.00164	0.00576	
16.2	0.0023	0.0063	
18.9	0.00238	0.0063	
21.6	0.00438	0.00715	
24.3	0.00576	0.00784	
27	0.007	0.01	First hairline crack appeared (100KN)
29.7	0.0073	0.011	
32.4	0.00746	0.013	
35.1	0.00923	0.014	
37.8	0.0115	0.015	
40.5	0.0126	0.0176	
43.2	0.0182	0.02	
48.6			Ultimate load(188KN)

3.7.1.6 BEAM NO.5

Beam wrapped with 10cm Bidirectional GFRP (90°)



Fig. 3.28 Beam 5 after testing



Fig. 3.29 Crack appeared between GFRP strips in Beam 5



Fig. 3.30 Magnified picture of crack developed between GFRP strips in Beam 5



Fig. 3.31 Crack developed Under GFRP strips in Beam 5

Table 3.10 Relation between angle of twist and Torsional moment of Beam 5

Torsional moment (knm)	Angle of twist (rad/m) (section-1)	Angle of twist (rad/m) (section-2)	Remarks
0.00	0.0000	0.0000	
2.70	0.0005	0.0019	
5.40	0.0010	0.0020	
8.10	0.0012	0.0021	
10.80	0.0015	0.0022	
13.50	0.0015	0.0022	
16.20	0.0017	0.0023	
18.90	0.0018	0.0025	
21.60	0.0019	0.0027	
24.30	0.0020	0.0028	
27.00	0.0022	0.0028	
29.70	0.0023	0.0030	
32.40	0.0025	0.0031	First hairline crack appeared (120KN)
35.10	0.0025	0.0032	
37.80	0.0026	0.0049	
40.50	0.0027	0.0059	
43.20	0.0027	0.0075	
45.90	0.0028	0.0092	
51.30	0.0034	0.0143	
58.05			Ultimate load(215KN)

3.7.1.7 BEAM NO.6

Beam wrapped with 5cm Unidirectional GFRP (90^0)



Fig. 3.32 Experimental Setup of the Beam 6



Fig. 3.33 Rupture of GFRP during testing of beam in Beam 6



Fig. 3.34 Crack pattern between GFRP sheets after testing in Beam 6

Table 3.11 Relation between angle of twist and Torsional moment of Beam 6

Torsional moment (KNm)	Angle of twist (rad/m) (section-1)	Angle of twist (rad/m) (section-2)	Remarks
0	0	0	
2.7	0.000769	0.000538	
5.4	0.000692	0.00058	
8.1	0.000615	0.000769	
10.8	0.000846	0.000769	
13.5	0.000846	0.00082	
16.2	0.000846	0.00095	
18.9	0.0013	0.00107	
21.6	0.0019	0.00146	First hairline crack appeared (80KN)
24.3	0.0023	0.002	
27	0.0025	0.0022	
29	0.0029	0.0023	
32.4	0.0032	0.00261	
35.1	0.00415	0.00338	
37.8	0.00469	0.0043	
40.5	0.00492	0.00538	Rupture and Debonding occurred
43.2	0.00569	0.007	
46.98			Ultimate load(174KN)

3.7.1.8 BEAM NO.7

Beam wrapped with 5cm Bidirectional GFRP (90°)



Fig. 3.35 Experimental Setup of the Beam 7



Fig. 3.36 Crack appeared during testing in Beam 7



Fig. 3.37 Rupture of GFRP occurred during testing in Beam 7



Fig. 3.38 Crack pattern under GFRP in Beam 7

Table 3.12 Relation between angle of twist and Torsional moment of Beam 7

Torsional moment (KNm)	Angle of twist (rad/m) (Section-1)	Angle of twist (rad/m) (Section-2)	Remarks
0	0	0	
2.7	0.0021	0.0032	
5.4	0.00234	0.0034	
8.1	0.00257	0.0039	
10.8	0.00269	0.0042	
13.5	0.00276	0.00434	
16.2	0.00261	0.00469	
18.9	0.00246	0.00492	
21.6	0.00246	0.00515	
24.3	0.00246	0.00576	
27	0.00284	0.00638	
29.7	0.003	0.00684	First hairline crack appeared (100KN)
32.4	0.00346	0.00784	
35.1	0.00376	0.00876	
37.8	0.00423	0.00992	
40.5	0.00569	0.011	
43.2	0.00684	0.0114	
45.5	0.00769	0.0118	Rupture and debonding occurred
48.6	0.00934	0.01278	
58.32			Ultimate load(216KN)

3.7.1.9 BEAM NO.8

Beam wrapped with 5cm Unidirectional GFRP (45°)



Fig. 3.39 Experimental Setup of the Beam 8



Fig. 3.40 Hairline Crack developed between GFRP strips in Beam 8



Fig. 3.41 Rupture of GFRP strips occurred during test in Beam 8



Fig. 3.42 Crack pattern under GFRP strips in Beam 8

Table 3.13 Relation between angle of twist and Torsional moment of Beam 8

Torsional moment (KNm)	Angle of twist (rad/m) (Section-1)	Angle of twist (rad/m) (Section-2)	Remarks
0	0	0	
2.7	0.002	0.002	
5.4	0.00484	0.0041	
8.1	0.0059	0.0053	
10.8	0.0073	0.00615	
13.5	0.0085	0.007	
16.2	0.0099	0.00784	
18.9	0.011	0.00861	
21.6	0.013	0.00915	
24.3	0.014	0.0099	First hairline crack appeared (90KN)
27	0.016	0.01	
29	0.018	0.011	
32.4	0.019	0.012	
35.1	0.02	0.0126	
37.8	0.022	0.013	
40.5	0.023	0.0138	
43.2	0.024	0.016	
45.5	0.025	0.019	Debonding Occurred
48.6	0.028	0.021	
54			Ultimate load(200KN)

3.7.1.10 BEAM NO.9

Beam wrapped with 5cm Bidirectional GFRP (45°)



Fig. 3.43 Experimental Setup of the Beam 9



Fig. 3.44 Debonding of GFRP sheet in Beam 9



Fig. 3.45 Debonding of GFRP sheet in Beam 9



Fig. 3.46 Crack pattern under GFRP sheets in Beam 9

Table 3.14 Relation between angle of twist and Torsional moment of Beam 9

Torsional moment (KNm)	Angle of twist (rad/m) (Section-1)	Angle of twist (rad/m) (Section-2)	Remarks
0	0	0	
2.7	0.00176	0.001	
5.4	0.0023	0.00107	
8.1	0.0033	0.00143	
10.8	0.00384	0.00156	
13.5	0.00432	0.0016	
16.2	0.004671	0.0017	
18.9	0.00476	0.00187	
21.6	0.00481	0.0019	
24.3	0.0051	0.002	
27	0.00589	0.00231	
29.7	0.00624	0.00243	First hairline crack appeared (90KN)
32.4	0.00695	0.00247	
35.1	0.00715	0.00253	
37.8	0.00759	0.00268	
40.5	0.00783	0.00307	
43.2	0.00813	0.00423	
45.5	0.0093	0.00469	
48.6	0.011	0.00569	Debonding Occurred
51.3	0.0143	0.00746	
54.54			Ultimate load(200KN)

3.8 SUMMARY

This chapter gives the angle of twist of each beam after application of load in an increasing manner on the two moment arms of the beam. The failure pattern and ultimate load carrying capacity is discussed in the proceeding chapter.

CHAPTER 4

NUMERICAL ANALYSIS USING ANSYS

4.1 INTRODUCTION

The finite element method is a numerical analysis technique for obtaining approximate solutions to a wide variety of engineering problems. ANSYS is a general purpose finite element modelling package for numerically solving a wide variety of problems which include static/dynamic structural analysis (both linear and nonlinear), heat transfer and fluid problems, as well as acoustic and electro-magnetic problems. The Rectangular beams with tensile reinforcement and shear reinforcement have been analyzed using a finite element (FE) model in ANSYS. Here, a linear analysis is considered throughout the study by assuming that there is a perfect bonding between reinforcement and the steel.

4.2 FINITE ELEMENT MODELLING

4.2.1 Reinforced Concrete

SOLID65 is used for the 3-D modelling of solids with or without reinforcing bars (rebar). The solid is capable of cracking in tension and crushing in compression. In concrete applications, for example, the solid capability of the element may be used to model the concrete while the rebar capability is available for modelling reinforcement behaviour. Other cases for which the element is also applicable would be reinforced composites (such as fibreglass), and geological materials (such as rock). The element is defined by eight nodes having three degrees of freedom at each node: translations in the nodal x, y, and z directions. Up to three different rebar specifications may be defined.

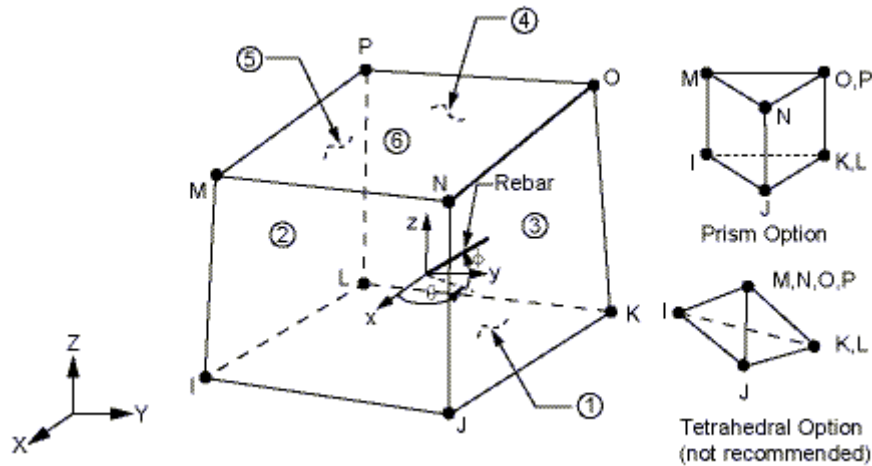


Fig. 4.1 SOLID65 element

4.2.2 Steel Reinforcement

To model concrete reinforcing, discrete modelling is used by assuming that bonding between steel and concrete is 100 percent. BEAM188 is used as reinforcing bars, it is a quadratic beam element in 3-D. BEAM188 has six degrees of freedom at each node. These include translations in the x, y, and z directions and rotations about the x, y, and z directions. This element is well-suited for linear, large rotation, and/or large strain nonlinear applications.

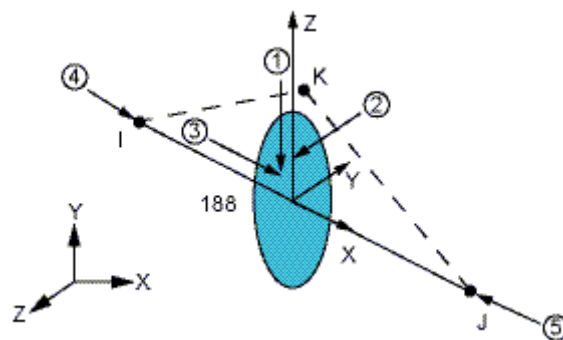


Fig. 4.2 BEAM188 element

4.2.3 Steel Plates

To model supports and under the load steel plate is used, which SOLID 45 is used, it is used for the 3-D modelling of solid structures. The element is defined by eight nodes having three degrees of freedom at each node: translations in the nodal X, Y, and Z directions. The element has plasticity, creep, swelling, stress stiffening, large deflection, and large strain capabilities.

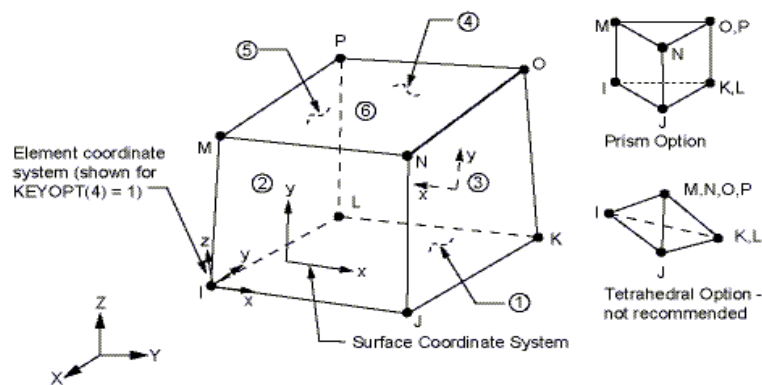


Fig. 4.3 SOLID45 element.

4.2.4 Laminates

To model laminated composites SHELL 91 is used. It may be used for layered applications of a structural shell model or for modelling thick sandwich structures. Up to 100 different layers are permitted for applications with the sandwich option turned off. When building a model using an element with *fewer* than three layers, SHELL 91 is more efficient than SHELL 99.

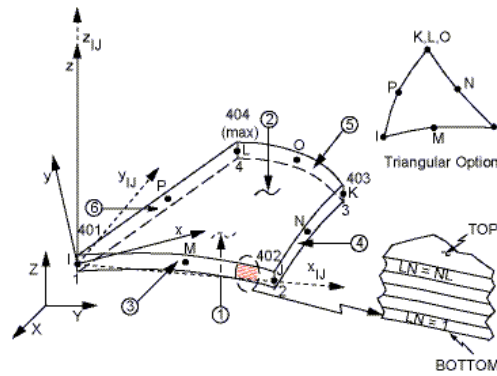


Fig. 4.4 SHELL91 element.

4.3 MATERIAL PROPERTIES

Linear analysis is considered for modelling of the beams, Table 4.1 summarizes the material linear properties and elements used in the modelling.

Table 4.1 Material properties and elements used in the modelling.

Materials	Density (kg/m ³)	Elastic Modulus (MPa)	Poisson's ratio	Fc28 (MPa)	Fy (MPa)	Element Used
Concrete	2400	19364	0.17	15	-	SOLID65
Reinforcing Steel	7850	210000	0.27	-	415	BEAM188
Steel Plate	7850	210000	0.27	-	415	SOLID45

4.4 GEOMETRY AND LOADING CONDITIONS

Simply supported beam is considered having and overall length of 1650 mm with effective length of 1600 mm. Size of the beam is 150 x 250 mm. Figure 5.5 shows the control beam with boundary conditions used in the analysis. Two points loading is applied at the two moment arms of the main beam which are 270mm away from main beam. These moment arm are used to give the twisting to the main beam. To get the accuracy of results mesh size considered as 25 mm as edge length.

High-Yield Strength Deformed bars of 16 mm and 10 mm diameter are used for the longitudinal reinforcement and 8 mm diameter bars are used as stirrups. For the moment arm part of the beam 12 mm and 10 mm diameter bars are used for longitudinal reinforcement. The tension reinforcement consists of 2 no's 16 mm diameter HYSD bars. Three bars of 12 mm of HYSD bars are provided on the top of the moment arm .The detailing of reinforcement of the beam is shown in figure 5.6 and figure 5.7 shows the deep beam model with FRP.

Total four numbers of beams were modelled in ANSYS. Series-3 and series-4 beams were modelled for this ANSYS modelling.

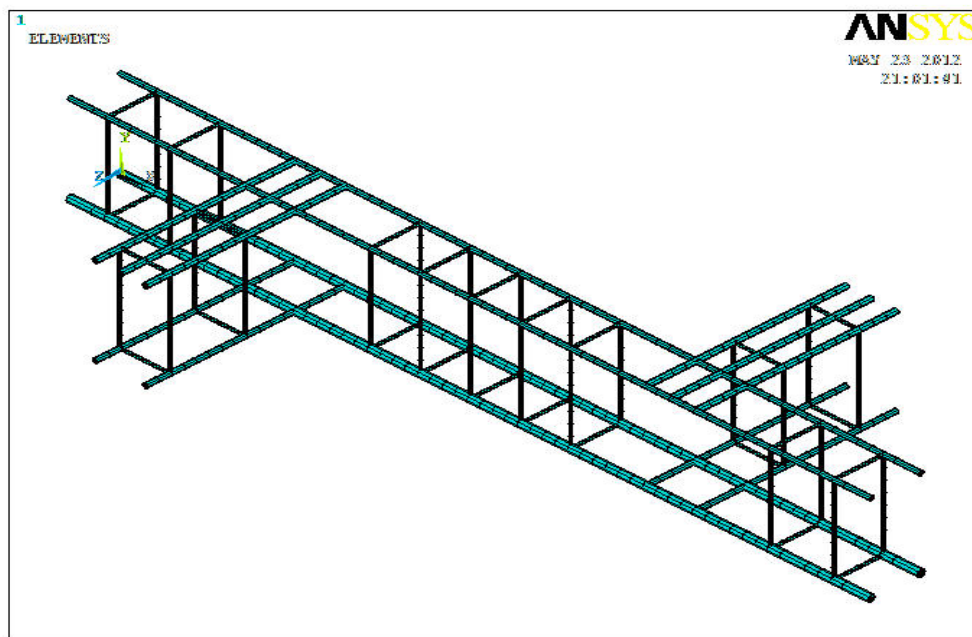


Fig. 4.5 Reinforcement model in ANSYS.

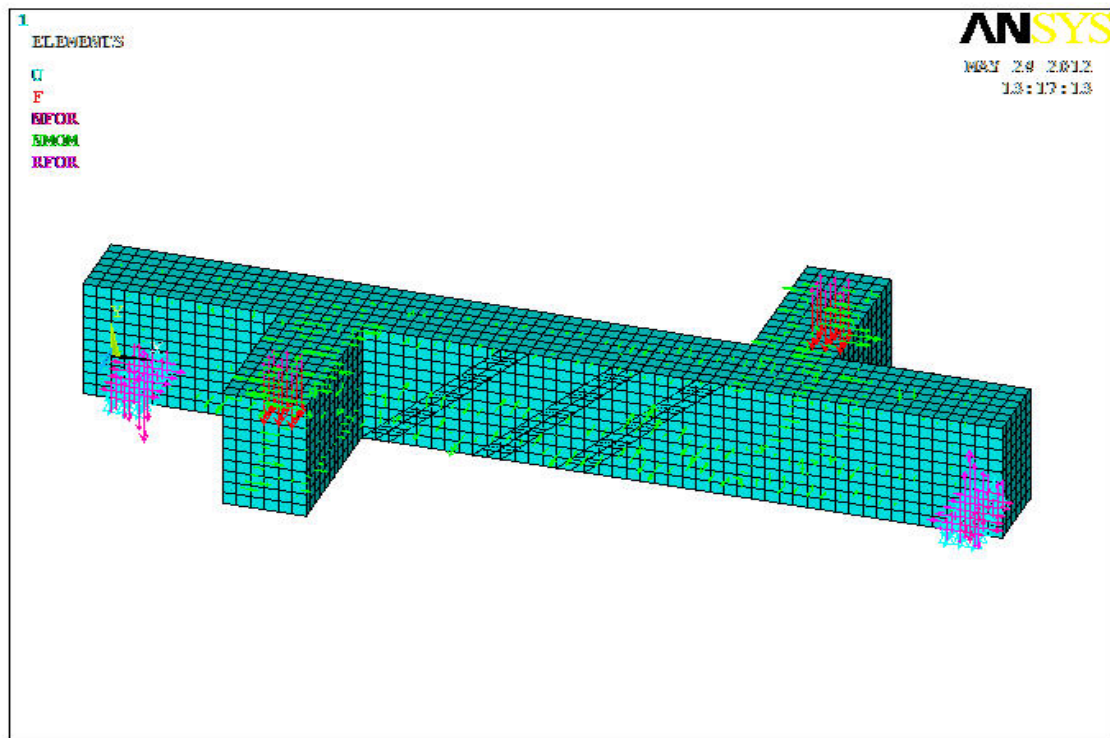


Fig. 4.6 Beam model in ANSYS with FRP making 45°

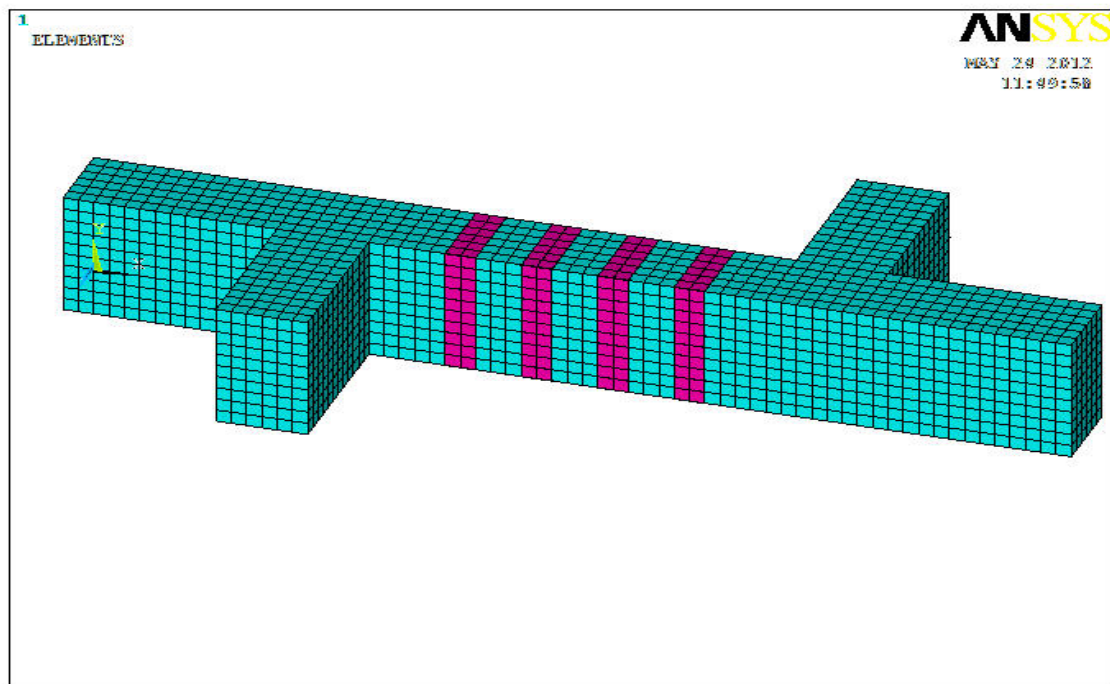


Fig. 4.7 Beam model with FRP in ANSYS with FRP making 90°

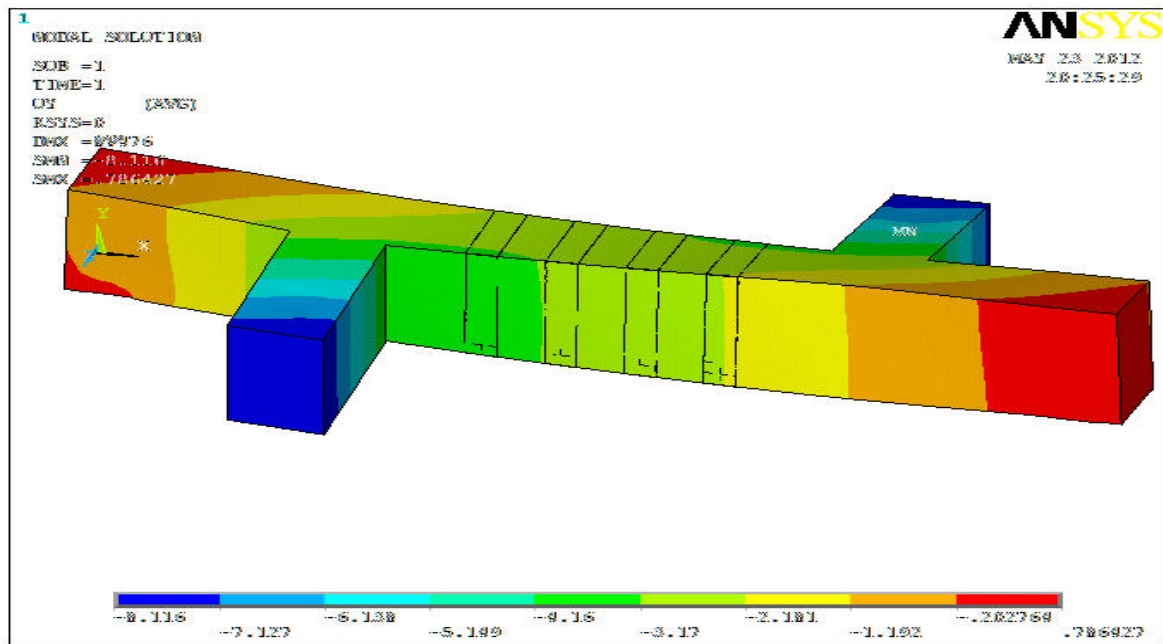


Fig. 4.8 Deflected shape of Beam model in ANSYS

CHAPTER 5

RESULTS AND DISCUSSIONS

5.1 EXPERIMENTAL RESULTS

This chapter includes all the experimental results of all beams with different types of configurations and orientation of GFRP. Their behavior throughout the test is described using recorded data on torsional behavior and the ultimate load carrying capacity. The crack patterns and the mode of failure of each beam are also described in this chapter. All the beams are tested for their ultimate strengths. Beam No-1 is taken as the control beam. It is observed that the control beam had less load carrying capacity and high deflection values compared to that of the externally strengthened beams using GFRP sheets.

All the eight beams except the control beam are strengthened with GFRP sheets in different patterns. In series-1 two beams were fully wrapped, one with unidirectional GFRP and other with bidirectional GFRP. In series-2 two beams were wrapped with 10cm wide GFRP sheets, one with unidirectional GFRP and other with bidirectional GFRP. In series-3 two beams were wrapped with 5cm GFRP sheets, one with unidirectional GFRP and other with bidirectional GFRP. In series-4 two beams were wrapped with 5cm GFRP sheets, one with unidirectional GFRP and other with bidirectional GFRP making 45^0 with the main beam.

5.2 FAILURE MODES

Different failure modes have been observed in the experiments of rectangular RC beams strengthened in torsion by GFRPs.

These include shear failure due to GFRP rupture .Rupture of the FRP strips is assumed to occur if the strain in the FRP reaches its design rupture strain before the concrete reaches its maximum usable strain. GFRP debonding can occur if the force in the FRP cannot be sustained by the substrate. In order to prevent debonding of the GFRP laminate, a limitation should be placed on the strain level developed in the laminate. Load was applied on the two moment arm of the beams which is 0.27m away from the main beam and at the each increment of the load, deflections at $L/3$, $L/2$ and $2L/3$ is taken with the help of dial gauges. Mid section at $L/2$ was taken as sec-1 and section 300mm away from sec-1 was taken as section 2.The load arrangement was same for all the beams.

The control beam and GFRP strengthened beam are tested to find out their ultimate load carrying capacity. It is found that all the beams failed in torsional shear.

Beam-2 continuously fully wrapped with unidirectional fabric did not show any failure in the strengthen part but the unstrengthen cantilever arm transferring moment had failed. Similarly Beam-3 continuously fully wrapped with biidirectional fabric did not show any failure in the strengthen part but the unstrengthen cantilever arm transferring moment had failed. In both cases failure is partial.

Beam-4 & Beam-5 continuously fully wrapped with strips of 10 cm of uni and bi directional fabrics failure occurred in the unstrengthen part. The failure is due to combination of shear and torsion in the region. The diagonal cracks initiated from the concrete portion in between the strips and propagated in the concrete below the fabrics. There was no deboning of GFRP fabrics.

All the beams of series 3 & 4 showed similar types of failure pattern. The failure occurred due to rupture of GFRP fabrics occurred generally at bottom face due to combined action of flexure and torsion. The diagonal cracks developed between the stripes of 5cm width.

5.3 TORSIONAL MOMENT AND ANGLE OF TWIST ANALYSIS

5.3.1 Torsional moment and Angle of twist Analysis of all Beams

Here the angle of twist of each beam is analyzed. Angle of twist of each beam is compared with the angle of twist of control beam. Also the torsional behaviour is compared between different wrapping schemes having the same reinforcement. Same type of load arrangement was done for all the beams.

All the beams were strengthened by application of GFRP in two layers over the beams. It was noted that the behaviour of the beams strengthen with GFRP sheets are better than the control beams. The deflections are lower when beam was wrapped externally with GFRP sheets. The use of GFRP sheet had effect in delaying the growth of crack formation.

When all the wrapping schemes are considered it was found that the Beam-2 with GFRP sheet fully wrapped over full a length of 0.65m in the middle part had a better resistant to torsional behaviour as compared to the others strengthened beams with GFRP.

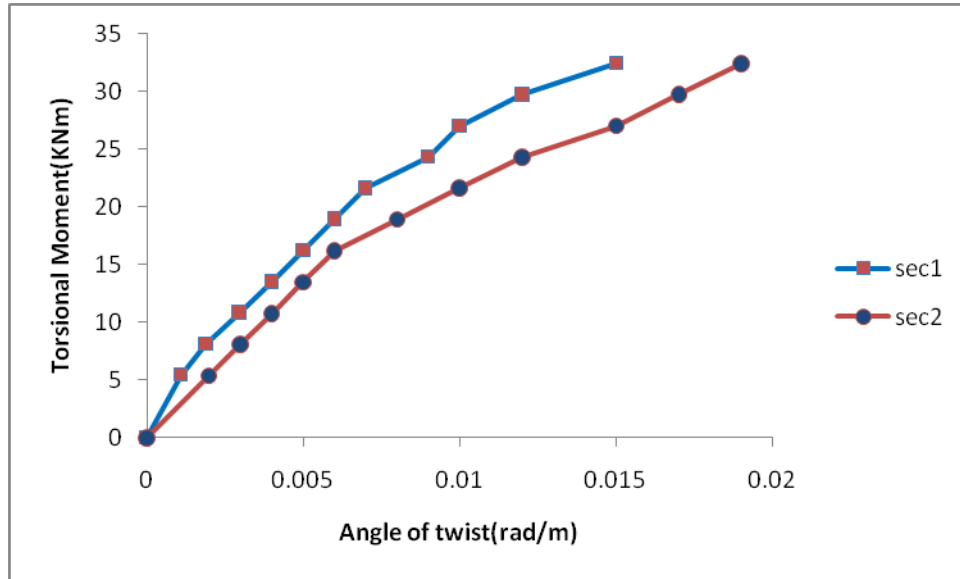


Fig. 5.1 Torsional Moment vs. Angle of Twist Curve for Control Beam-1

Beam 1 is taken as the control beam which is weak in torsion. In Beam1 no strengthening is done. Load was applied on the two moment arm of the beams which is 0.27m away from the main beam and at the each increment of the load, deflection at $L/3$, $L/2$ and $2L/3$ is taken with the help of dial gauges. Using this load and deflection data, the corresponding torsion moment and the twisting angle were calculated and the above graph was plotted.

At the load of 80 KN initial hairline cracks appeared. Later with the increase in loading values the crack propagated further. The Beam1 failed completely in torsion at a load 130KN and torsional moment 35.1KNm. It was observed those cracks were appeared making an angle 40^0 - 50^0 with the main beam. The cracks were developed in a spiral pattern all over the main beam which later leads to the collapse of the beam in torsional shear.

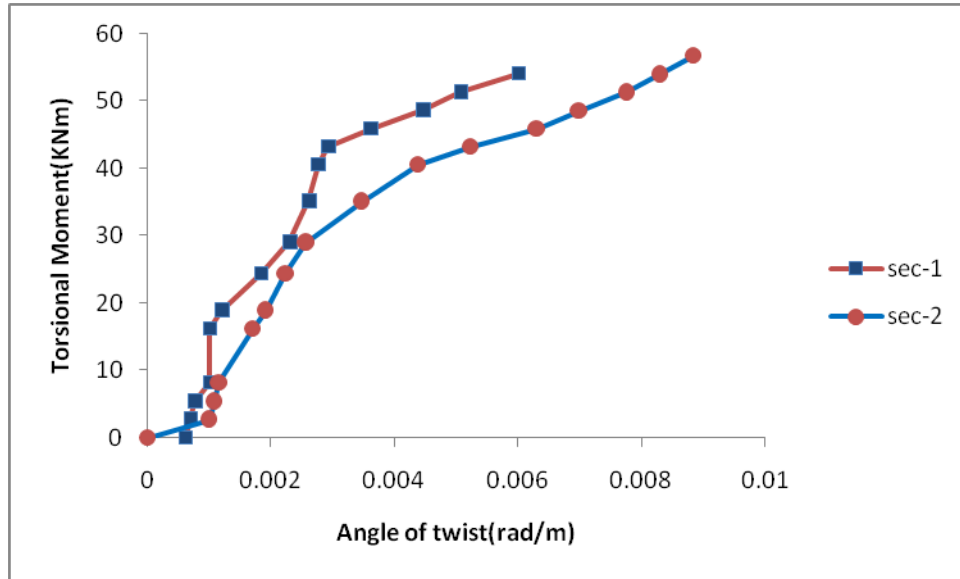


Fig. 5.2 Torsional Moment vs. Angle of Twist Curve for Beam-2

Beam-2 was strengthened by wrapping the full span of the beam under torsion with unidirectional GFRP. Using the load and deflections data from experiment, the corresponding torsion moment and the twisting angle were calculated and the above graph was plotted.

At the load of 100 KN cracking sound was heard. The Beam 2 failed completely in torsion at a load 245KN and torsional moment 66.15KNm. The increase strength of beam was 88.46% as compared to control beam. After the test is done the GFRP sheets were removed and the crack pattern was observed. It was found that the crack were appeared making an angle 45° - 50° with the main beam on the side faces and top surface.

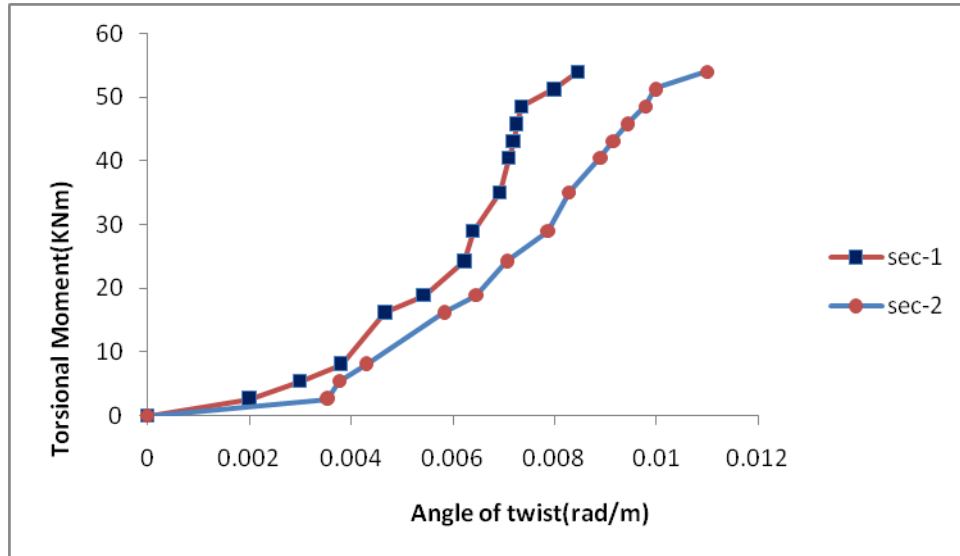


Fig. 5.3 Torsional Moment vs. Angle of Twist Curve for Beam-3

Beam-3 was strengthened by fully wrapping the span of the beam under torsion with bidirectional GFRP. Using the loads and deflections data from experiment, the corresponding torsion moment and the twisting angle were calculated and the above graph was plotted. At the load of 140 KN cracking sound was heard. The Beam 3 failed completely in torsion at a load 210KN and torsional moment 56.7KNm. After the test is done the GFRP sheets were removed and the crack pattern was observed. It was found that the crack were appeared making an angle 50° - 60° with the main beam on the side faces and top surface.

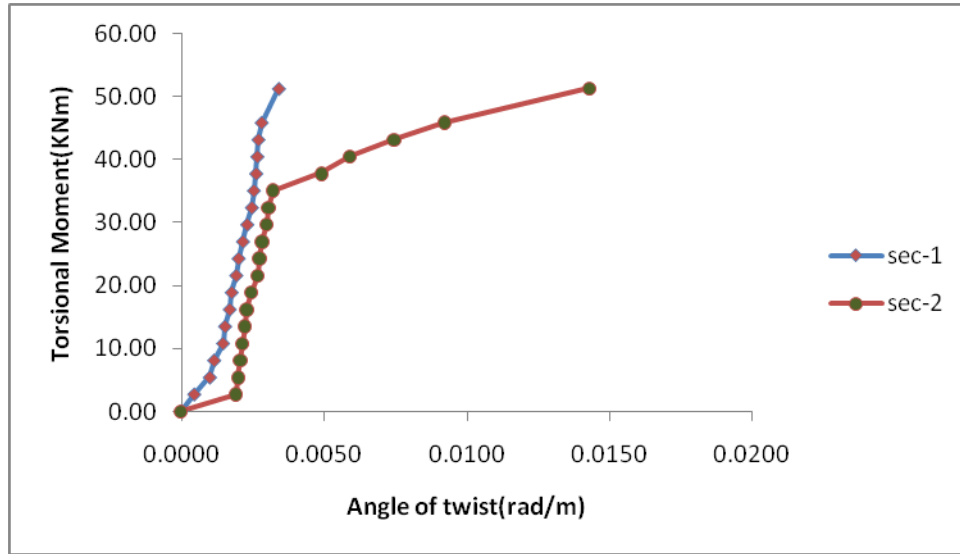


Fig. 5.4 Torsional Moment vs. Angle of Twist Curve for Beam-4

Beam-4 was strengthened by wrapping with four 10cm Unidirectional GFRP strips at a distance 8.3cm from each other over the beam under torsion. Using the loads and deflections data from experiment, the corresponding torsion moment and the twisting angle were calculated and the above graph was plotted.

At the load of 140 KN cracking sound was heard. The Beam 3 failed completely in torsion at a load 210KN and torsional moment 56.7kNm. The increase strength of beam was 61.53% as compared to control beam. After the test is done the GFRP sheets were removed and the crack pattern was observed. It was found those cracks were appeared making an angle 60° with the main beam on the side faces and top surface.

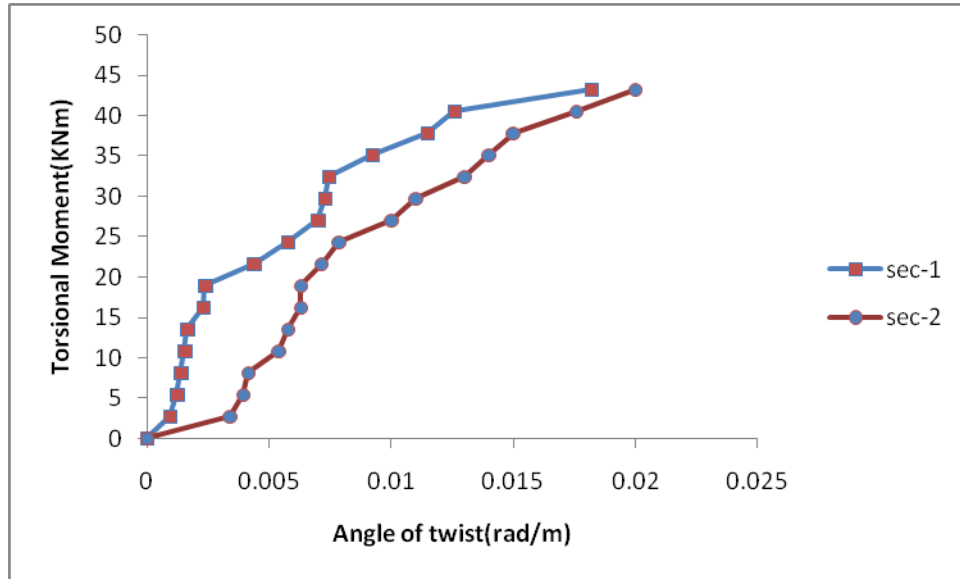


Fig. 5.5 Torsional Moment vs. Angle of Twist Curve for Beam-5

Beam-5 was strengthened by wrapping with four 10cm Bidirectional GFRP strips at a distance 8.3cm from each other over the beam under torsion. Using the loads and deflections data from experiment, the corresponding torsion moment and the twisting angle were calculated and the above graph was plotted.

At the load of 100 KN cracking sound was heard. The Beam 3 failed completely in torsion at a load 188KN and torsional moment 50.76KNm. The increase strength of beam was 44.61% as compared to control beam. After the test is done the GFRP sheets were removed and the crack pattern was observed. It was found those cracks were appeared making an angle 55° - 60° with the main beam on the side faces and top surface.

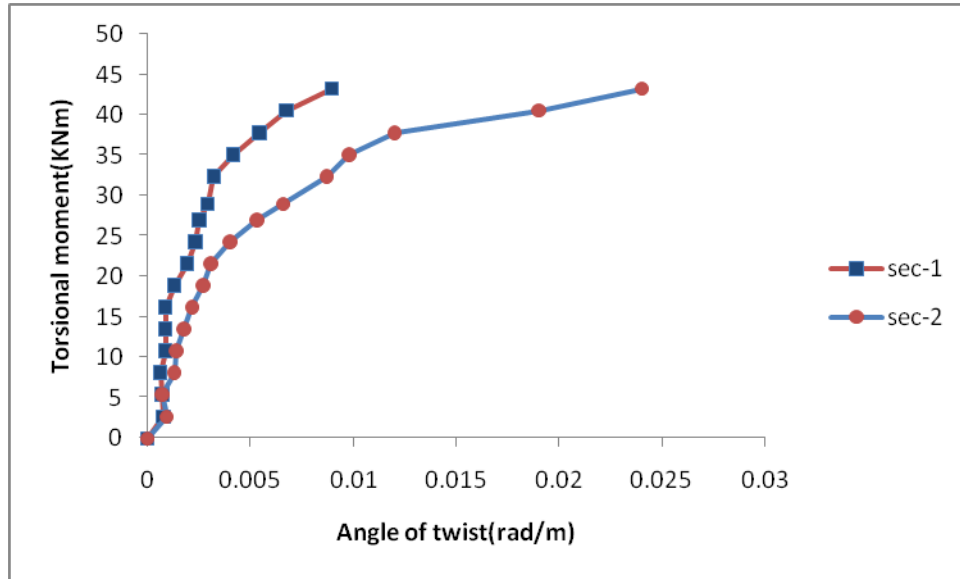


Fig. 5.6 Torsional Moment vs. Angle of Twist Curve for Beam-6

Beam-6 was strengthened by wrapping with four 5cm Unidirectional GFRP strips at a distance 15cm from each other over the beam under torsion. Using the loads and deflections data from experiment, the corresponding torsion moment and the twisting angle were calculated and the above graph was plotted.

At the load of 80 KN cracking sound was heard. The Beam 3 failed completely in torsion at a load 174KN and torsional moment 46.98KNm. The increase strength of beam was 65.38% as compared to control beam. After the test is done the GFRP sheets were removed and the crack pattern was observed. It was found those cracks were appeared making an angle 50° with the main beam on the side faces and top surface.

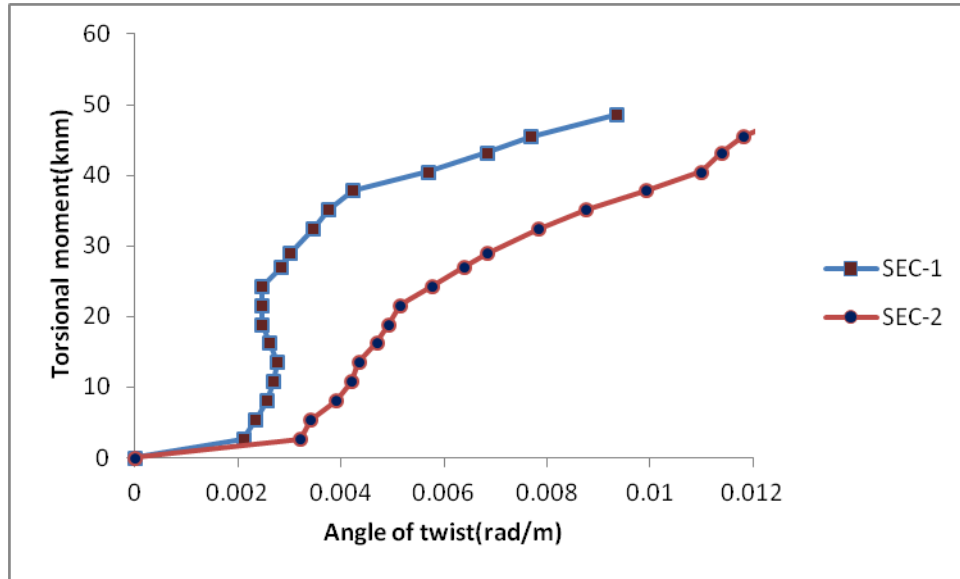


Fig. 5.7 Torsional Moment vs. Angle of Twist Curve for Beam-7

Beam-7 was strengthened by wrapping with four 5cm Bidirectional GFRP strips at a distance 15cm from each other over the beam under torsion. Using the load and deflection data from experiment, the corresponding torsion moment and the twisting angle were calculated and the above graph was plotted.

At the load of 100 KN cracking sound was heard. The Beam 3 failed completely in torsion at a load 216KN and torsional moment 58.32KNm. The increase strength of beam was 66.15% as compared to control beam. After the test is done the GFRP sheets were removed and the crack pattern was observed. It was found those cracks were appeared making an angle 55° - 65° with the main beam on the side faces and top surface.

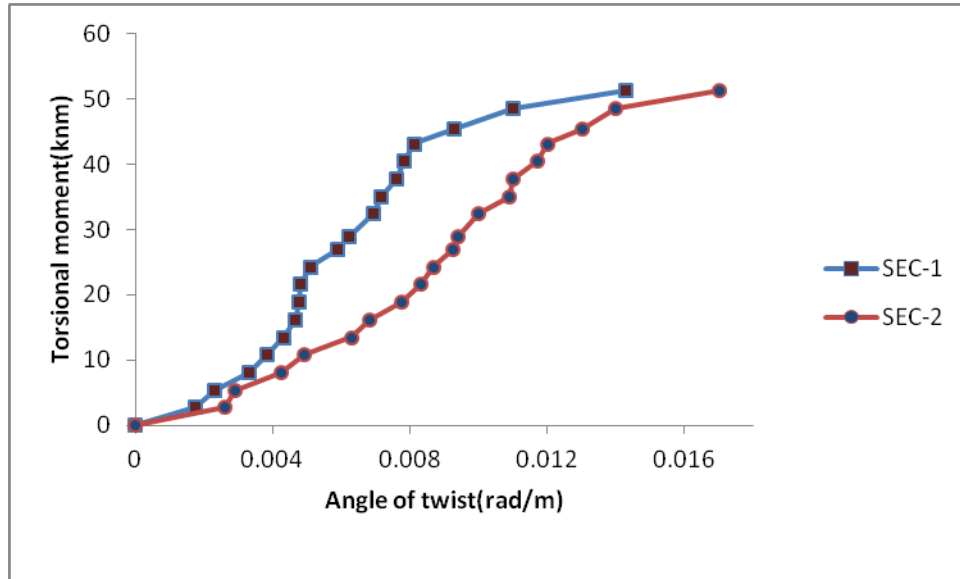


Fig. 5.8 Torsional Moment vs. Angle of Twist Curve for Beam-8

Beam-8 was strengthened by wrapping with four 5cm Bidirectional GFRP strips at a distance 15cm from each other over the beam under torsion. The GFRP strips were wrapped over the beam by making an angle 45° with the main beam. Using this loads and deflections data from experiment, the corresponding torsion moment and the twisting angle were calculated and the above graph was plotted.

At the load of 110 KN cracking sound was heard. The Beam 3 failed completely in torsion at a load 202KN and torsional moment 54.54KNm. The increase strength of beam was 53.84% as compared to control beam. After the test is done the GFRP sheets were removed and the crack pattern was observed. It was found those cracks were appeared making an angle 70° with the main beam on the side faces and 60° at the top surface.

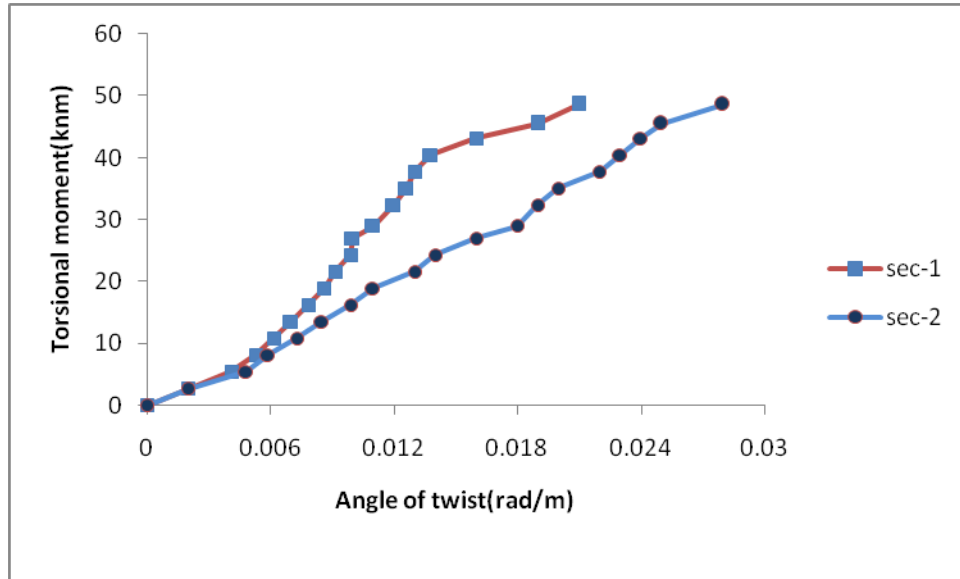


Fig. 5.9 Torsional Moment vs. Angle of Twist Curve for Beam-9

Beam-9 was strengthened by wrapping with four 5cm Bidirectional GFRP strips at a distance 15cm from each other over the beam under torsion. The GFRP strips were wrapped over the beam by making an angle 45° with the main beam. Using the loads and deflection data from experiment, the corresponding torsion moment and the twisting angle were calculated and the above graph was plotted.

At the load of 100 KN cracking sound was heard. The Beam 3 failed completely in torsion at a load 188KN and torsional moment 50.76KNm. The increase strength of beam was 55.38% as compared to control beam. After the test is done the GFRP sheets were removed and the crack pattern was observed. It was found those cracks were appeared making an angle 40° with the main beam on the side faces and 40° at the top surface.

It was observed from the test that with unidirectional fabrics cracks initiated making an angle between 40° to 60° with the axis of beam and with bidirectional fabrics steep cracks was developed by making an angle between 50° to 70° with the axis of the beam.

5.3.2 Torsional moment and Angle of twist Analysis of Beams Wrapped with Different Series of wrapping

Series-1 (Unidirectional & Bidirectional GFRP fully wrapped over the beam)

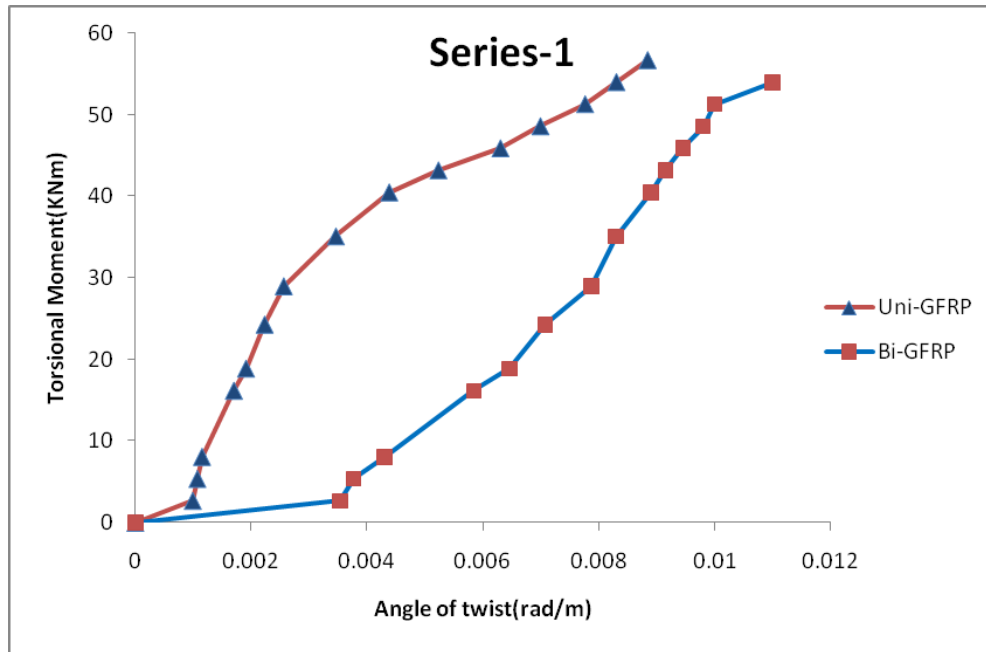


Fig. 5.10 Torsional Moment vs. Angle of Twist Curve for Beam-2 and Beam-3

Torsional reinforced concrete beams strengthened with GFRP sheets exhibited significant increase in their cracking and ultimate strength as well as ultimate twist deformations. Both, the Beam 2 & Beam 3 had partially collapsed without achieving the ultimate load. The failure occurred in the unstrengthened part of the specimens. The torsional strength of the retrofitted beams exceeded that of the control specimen by up to 88.46% for Beam 2 with unidirectional FRP and up to 61.5% for Beam 3 with bidirectional FRP. Test result reveals that strengthening using bidirectional GFRP sheets had not enhanced the ultimate strength but had increased the ductility of the beam.

Series-2 (Unidirectional & Bidirectional GFRP 10cm strips wrapped over the beam)

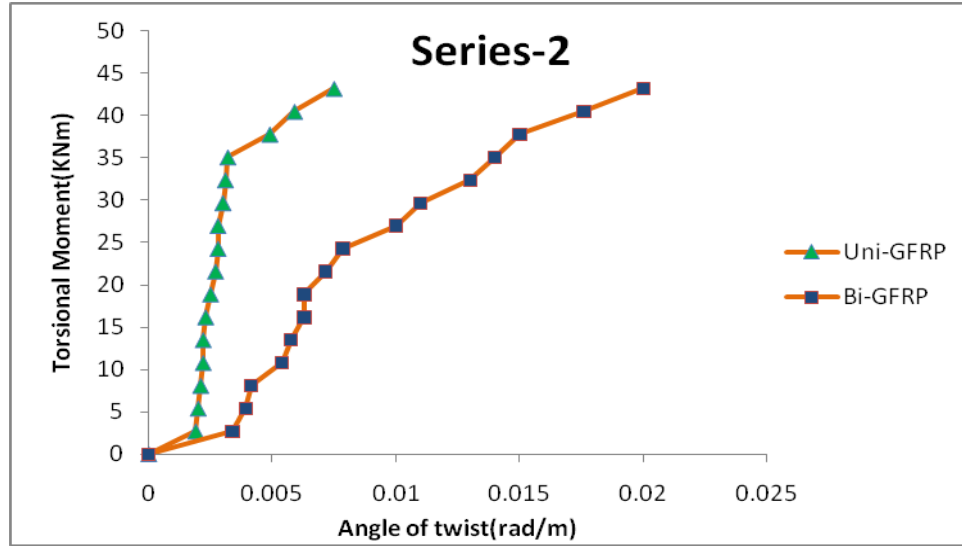


Fig. 5.11 Torsional Moment vs. Angle of Twist Curve for Beam-4 and Beam-5

The torsional strength of the retrofitted beams exceeded that of the control specimen by up to 44.61% for Beam 4 with unidirectional FRP and up to 65.38% for Beam 5 with bidirectional FRP. From the above graph it is observed that wrapping with Bidirectional GFRP is more efficient to arrest the crack and enhance the strength of the beam.

Series-3 (Unidirectional & Bidirectional GFRP 5cm strips wrapped over the beam)

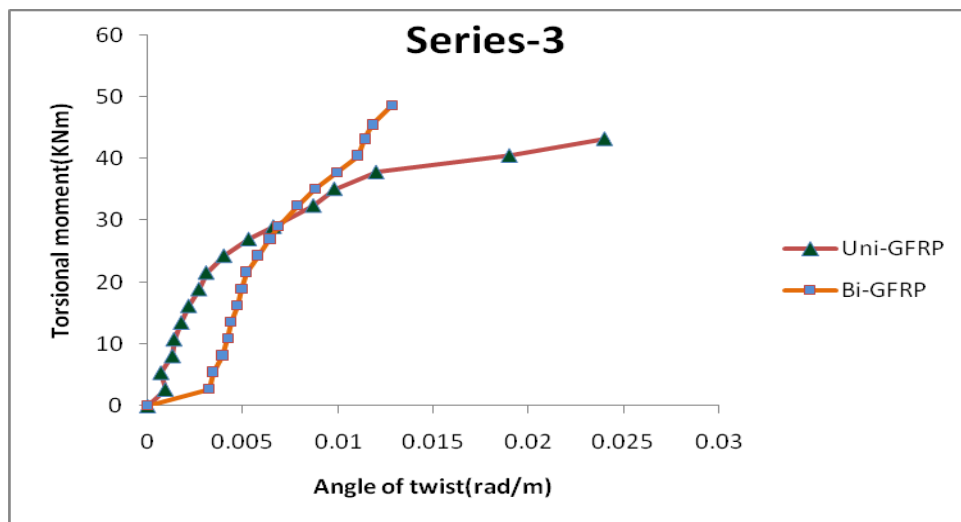


Fig. 5.12 Torsional Moment vs. Angle of Twist Curve for Beam-6 and Beam-7

Rupture and debonding of GFRP occurred in both of the beams. Both strips of Unidirectional and Bidirectional GFRP undergone rupture before ultimate failure of the beam. The torsional strength of the retrofitted beams exceeded that of the control specimen by up to 33.84% for Beam 6 with unidirectional FRP and up to 66.15% for Beam 7 with bidirectional FRP. From the above graph it is observed that wrapping with Bidirectional GFRP is more efficient to arrest the crack and enhance the strength of the beam.

Series-4 (Unidirectional & Bidirectional GFRP 5cm strips wrapped over the beam making an angle 45^0 with beam)

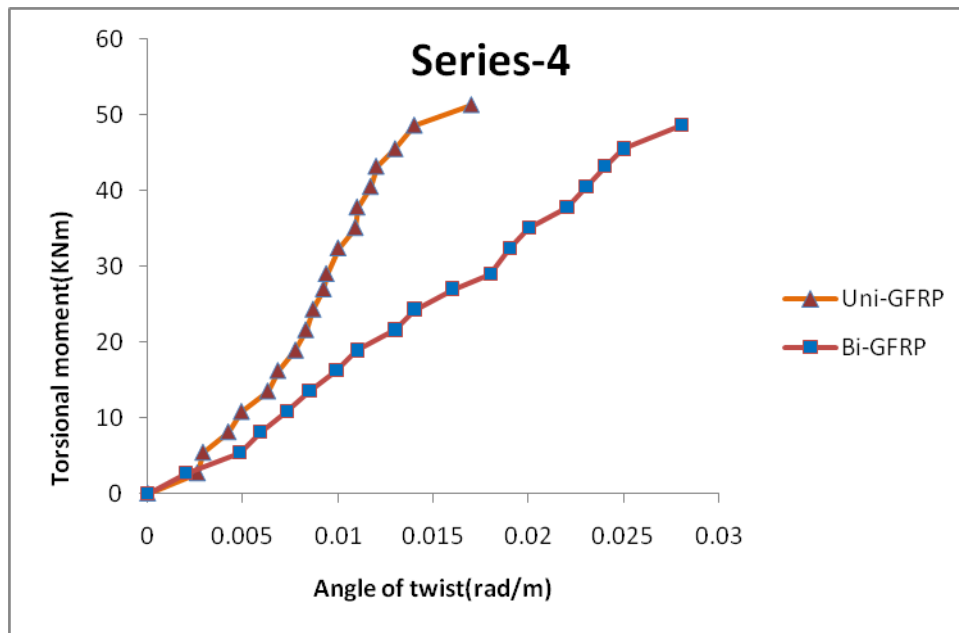


Fig. 5.13 Torsional Moment vs. Angle of Twist Curve for Beam-8 and Beam-9

Rupture and debonding of GFRP occurred in both of the beams. Both strips of Unidirectional and Bidirectional GFRP undergone rupture before ultimate failure of the beam. The torsional strength of the retrofitted beams exceeded that of the control specimen by up to 53.84% for Beam 8 with unidirectional FRP and up to 55.38% for

Beam 9 with bidirectional FRP. Both the beam 8 and Beam 9 were strengthened by applying the GFRP by making an angle 45^0 with the beam surface. From the above graph it is observed that wrapping with Bidirectional GFRP is more efficient to arrest the crack and enhance the strength of the beam if the beam is strengthened with GFRP at an angle 45^0 with the beam.

5.3.3 Torsional moment and Angle of twist Analysis of Beams Wrapped with Unidirectional GFRP

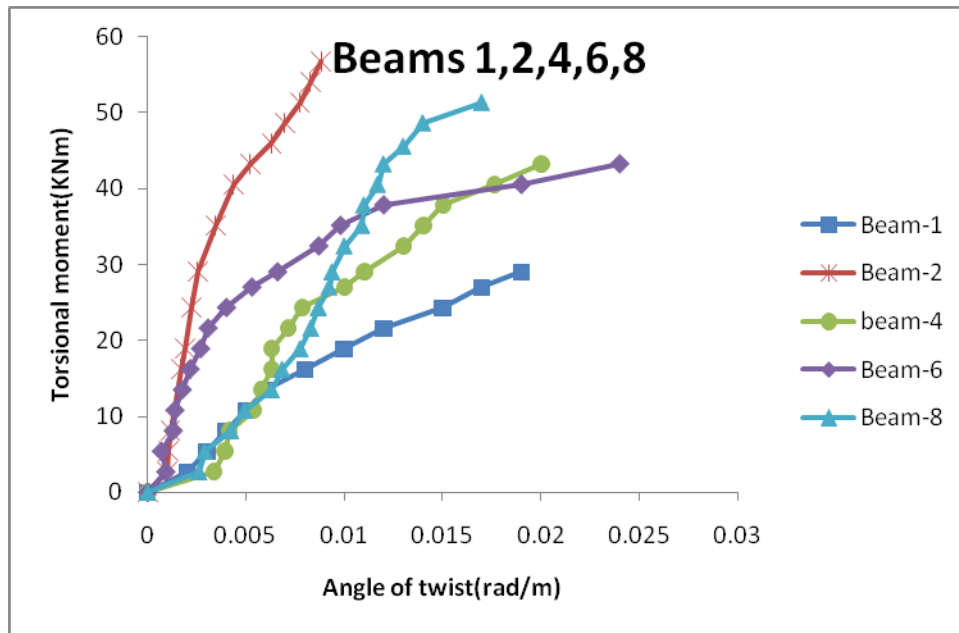


Fig. 5.14 Torsional Moment vs. Angle of Twist Curve for Beam-1, Beam-2, Beam-4, Beam-6 and Beam-8

Here all the beams strengthened with Unidirectional GFRP are compared with respect to their torsional moment and angle of twist. And it can be interpreted that beam 2 which was strengthened with full wrap double layered GFRP sheet for a length of 0.65 m in the main beam, a series of closely spaced cracks were visible on the concrete indicating torsional shear failure. And Beam 2 has the highest load carrying capacity among all the Beams strengthened with Uni-GFRP.

5.3.4 Torsional moment and Angle of twist Analysis of Beams Wrapped with Bidirectional GFRP

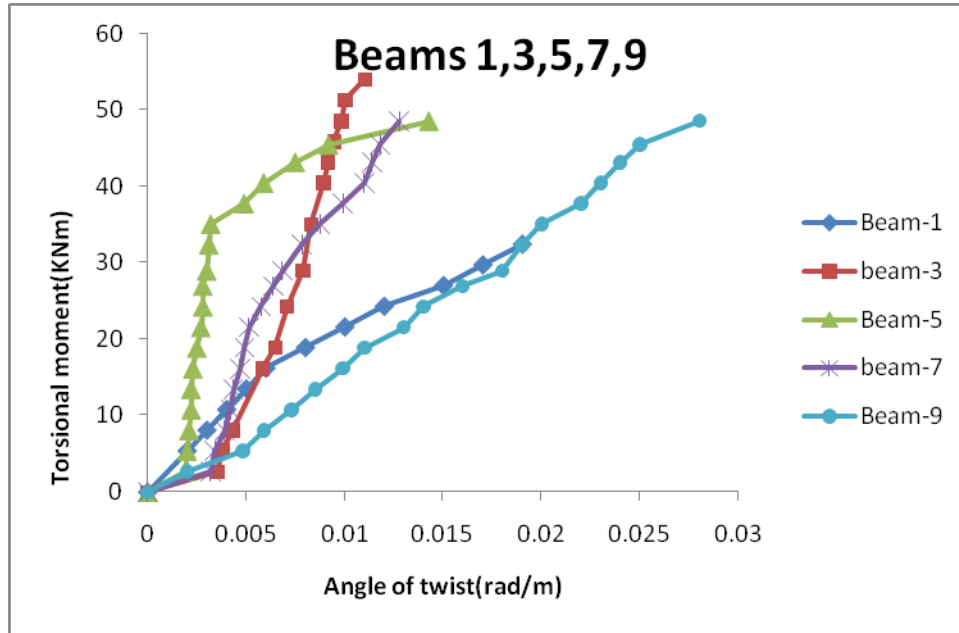


Fig. 5.15 Torsional Moment vs. Angle of Twist Curve for Beam-1, Beam-3, Beam-5, Beam-7 and Beam-9

Here all the beams strengthened with Bidirectional GFRP are compared with respect to their torsional moment and angle of twist. And it can be interpreted that beam 3 which was strengthened with full wrap double layered GFRP sheet for a length of 0.65 m in the main beam where most of the cracks are occurring has minimum angle of rotation value as compared to others. And Beam 3 has the highest load carrying capacity among all the Beams strengthened with Bi-GFRP.

5.3.5 Torsional moment and Angle of twist Analysis of All Beams

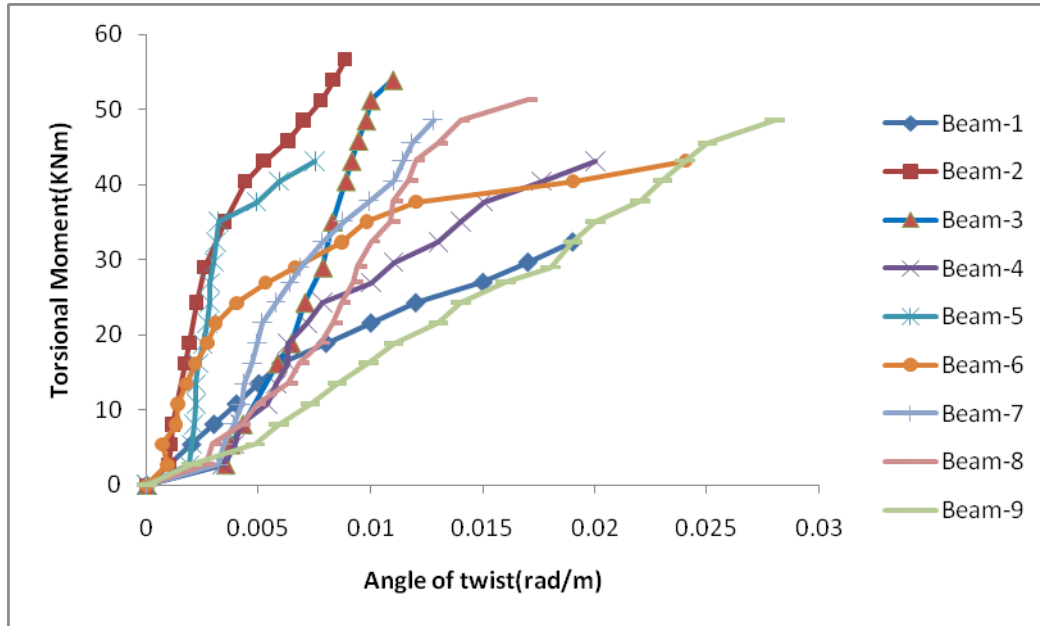


Fig. 5.16 Torsional Moment vs. Angle of Twist Curve for All Beams

In fig. 5.16 all the beams strengthened with Unidirectional GFRP are compared with respect to their torsional moment and angle of twist. And it can be interpreted that beam 2 which was strengthened with full wrap double layered GFRP sheet for a length of 0.65 m in the main beam gives the highest strength to the beam.

5.3.6 Load and angle of twist Analysis of Beams Wrapped with GFRP in Different Orientation

5.3.6.1 Beams Wrapped with Unidirectional GFRP at 90^0 and 45^0 angle making with Beam

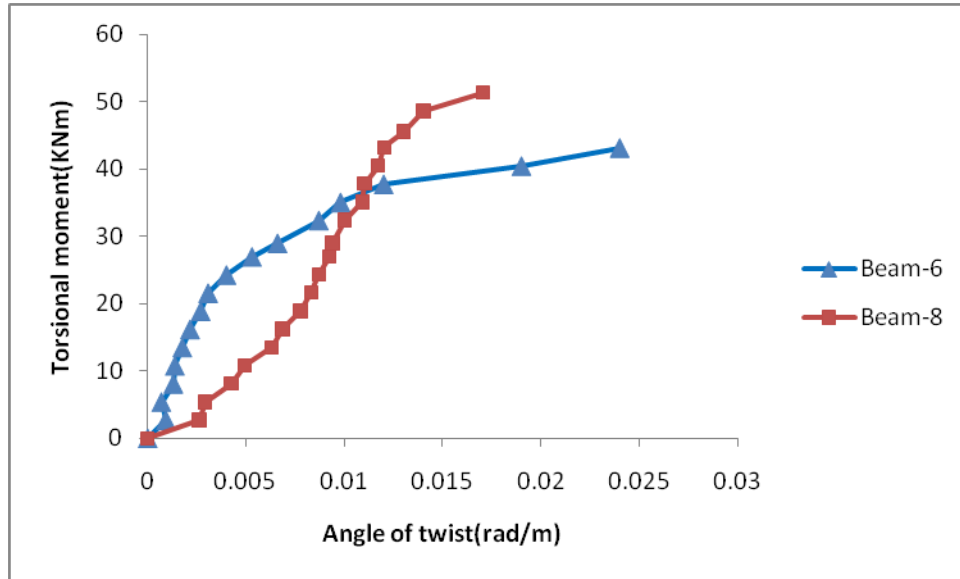


Fig. 5.17 Torsional Moment vs. Angle of Twist Curve for Beam-6 and Beam-8

5.3.6.2 Beams Wrapped with Bidirectional GFRP at 90^0 and 45^0 angle making with Beam

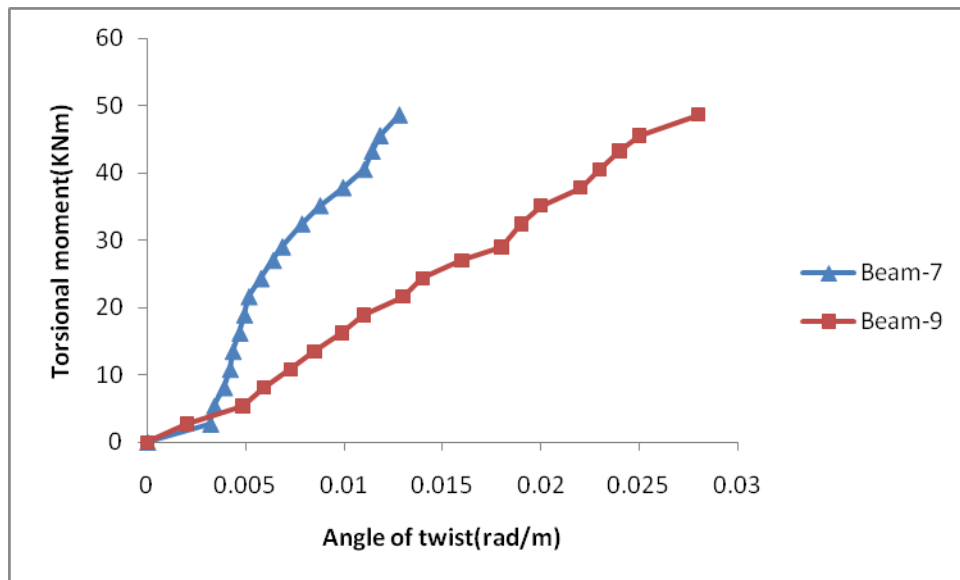


Fig. 5.18 Torsional Moment vs. Angle of Twist Curve Beam-7 and Beam-9

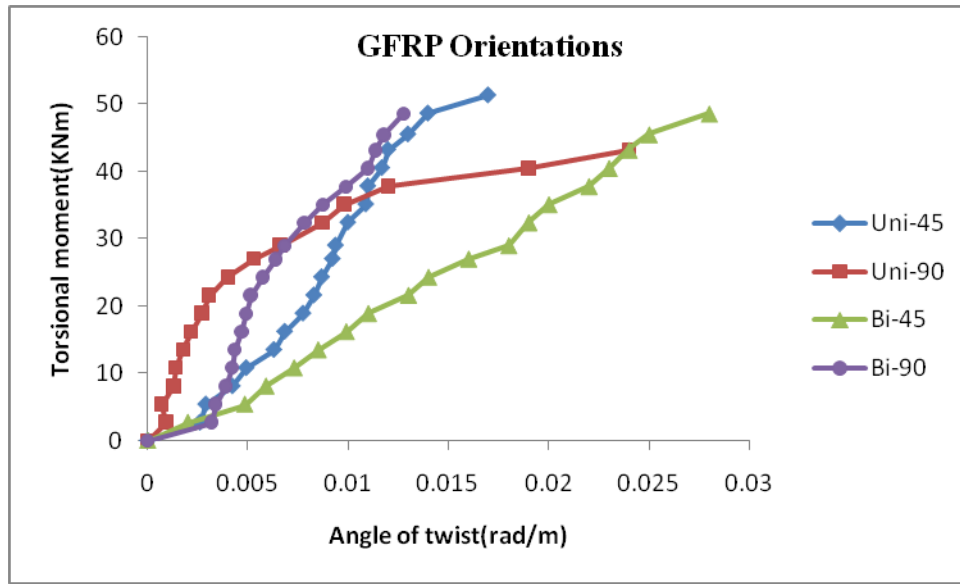


Fig. 5.19 Torsional Moment vs. Angle of Twist Curve for beams where GFRP applied in different orientations

From the above graph it can be observed that GFRP applied at an angle 45^0 to the beam gives more strength to the beam. Both Uni-GFRP and Bi-GFRP strips applied at 45^0 gives more strength to the beams compared to beam wrapped with Uni-GFRP and Bi-GFRP at an angle with 90^0 with the beam.

5.3.6.3 Load and angle of twist Analysis of Beams Wrapped with GFRP in Different Orientation Compared with ANSYS results

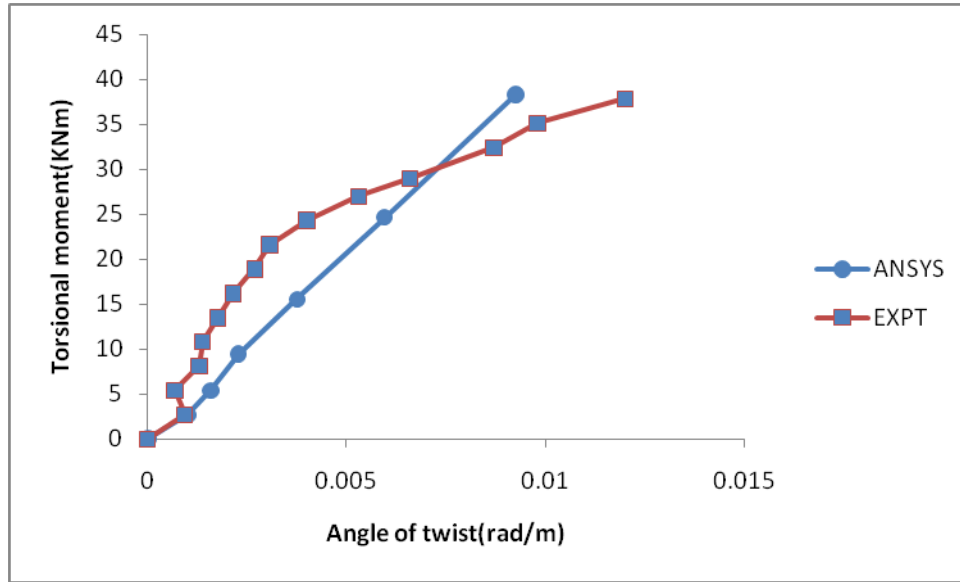


Fig. 5.20 Torsional Moment vs. Angle of Twist Curve for beams where Uni-GFRP applied at 90° orientations

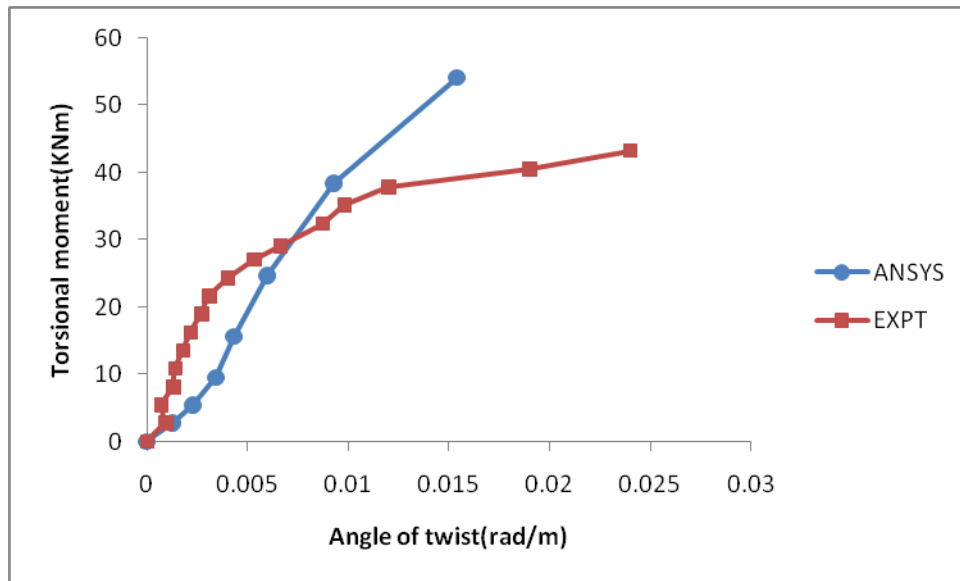


Fig. 5.21 Torsional Moment vs. Angle of Twist Curve for beams where Bi-GFRP applied at 90° orientations

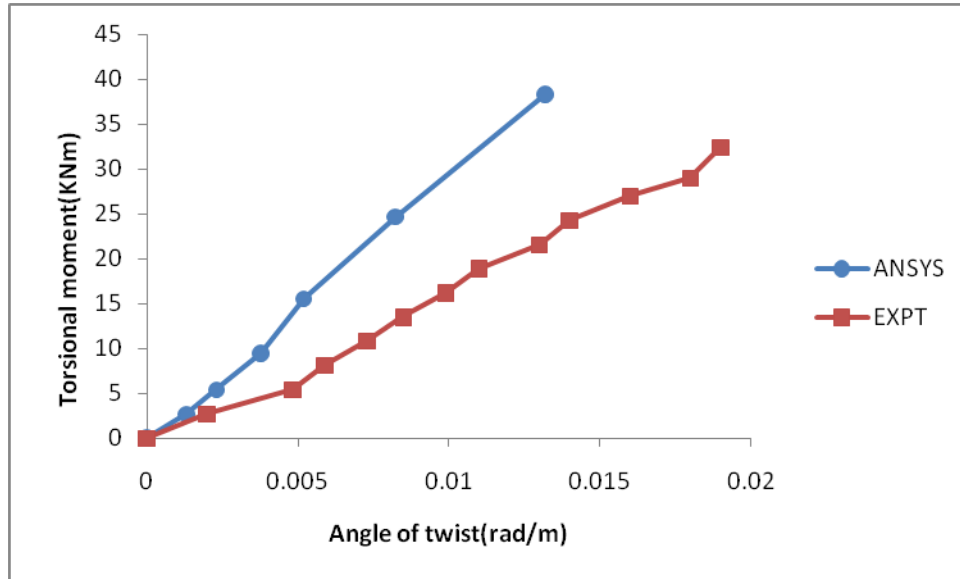


Fig. 5.22 Torsional Moment vs. Angle of Twist Curve for beams where Uni-GFRP applied at 45° orientations

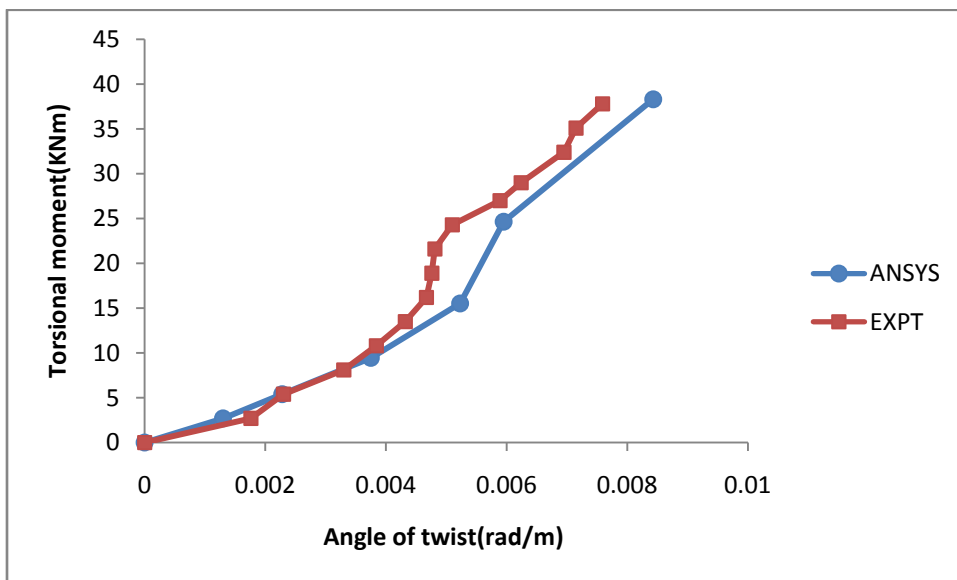


Fig. 5.23 Torsional Moment vs. Angle of Twist Curve for beams where Bi-GFRP applied at 45° orientations

The above graph shows that the angle of twist obtained using ANSYS matches the experimental results for lower range of load value for the beam which are wrapped with GFRP in 90° angles with main beam. For higher loads there is a deviation with experimental results for these beams. But for the experimental results obtained for beams wrapped with GFRP at an angle 45° with axis of the beam are in good agreement with ANSYS results.

The ultimate load carrying capacity of beams in series-3 and series-4 in ANSYS model was more as compared to the experimental results.

5.4 ULTIMATE LOAD CARRYING CAPACITY

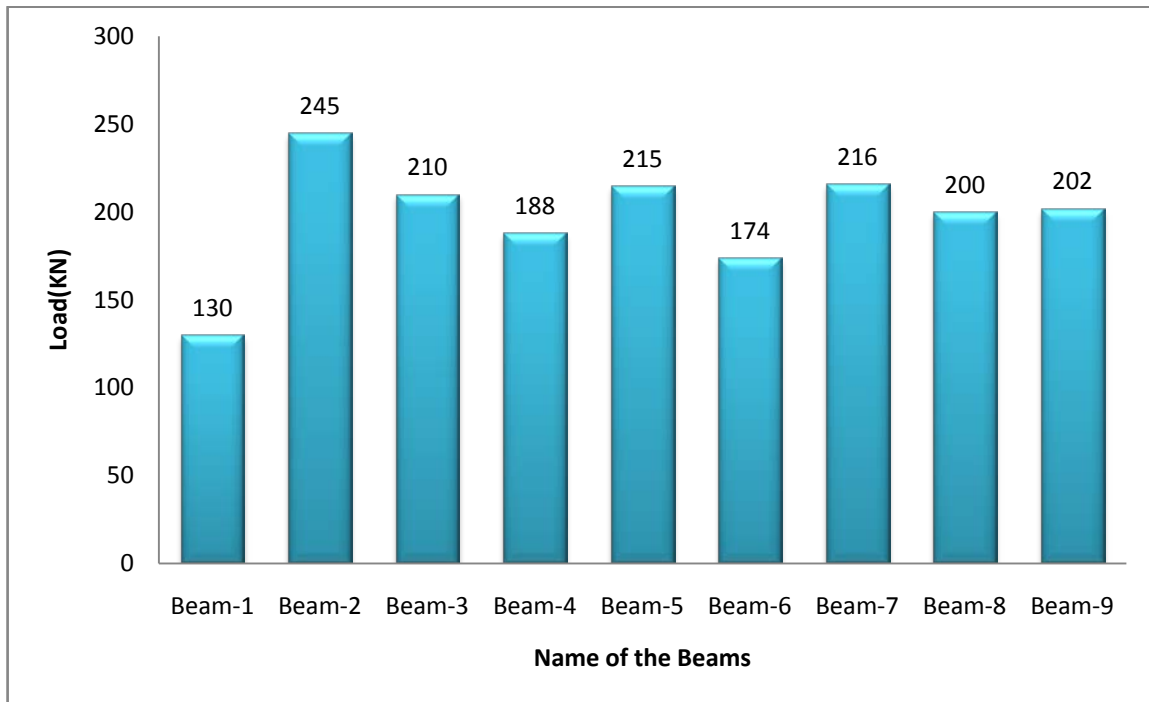


Fig. 5.24 Ultimate Load carrying capacity

In Fig.5.24 shows the load carrying capacity of the control beams and the strengthen beam are plotted below. It was observed that Beam 2 is having the max load carrying capacity.

5.4.1 Increase in load carrying capacity

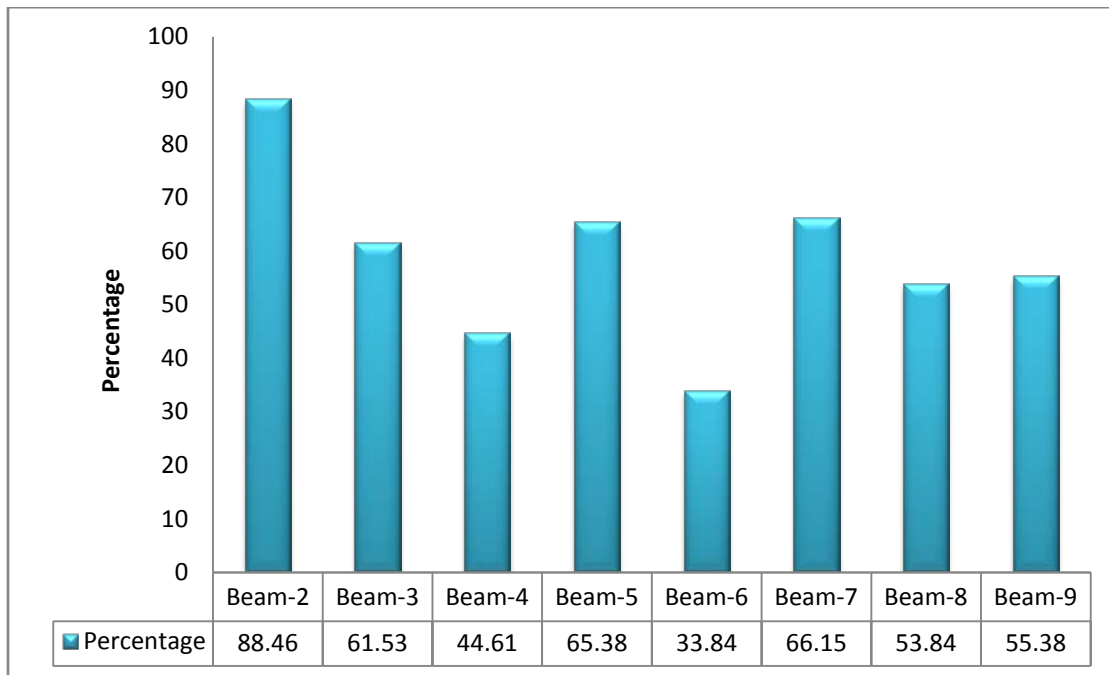


Fig. 5.25 Percentage increase in the Ultimate Carrying capacity w.r.t Control Beam 1

The above figure shows the amount of increase in the Torsional strength for each strengthened beam with respect to the Control Beam.

CHAPTER 6

CONCLUSIONS

6.1 CONCLUSIONS

The present experimental study is made on the torsional behaviour of rectangular RC beams strengthened by uni-directional and bi-directional GFRP fabrics. Nine rectangular RC beams having same reinforcement detailing and designed to fail in torsion and are cast and tested till collapse. During testing deflections and strain measurements are observed with the help of dial gauges and strain gauge. Following conclusions are drawn from the test results and calculated strength values:

1. The ultimate load carrying capacity of all the strengthen beams were enhanced as compared to the Control Beam1.
2. Torsional reinforced concrete beams strengthened with GFRP sheets exhibited significant increase in their cracking and ultimate strength as well as ultimate twist deformations.
3. Initial cracks appear for higher loads in case of strengthened beams.
4. The load carrying capacity of the strengthened Beam 2 fully wrapped with unidirectional fibre was found to be maximum of all the beams. The increase in load carrying capacity is 88.46% compared to control beam1.
5. Both fully wrapped beams Beam 2 and Beam 3 had partially collapsed without achieving the ultimate load. The failure occurred in the unstrengthened part of the specimens.
6. Beam 8 and Beam 9 were giving the best results in terms of load carrying capacity and angle of twist respectively. And both are having same wrapping pattern of GFRP which is bonded in the torsion part at an angle 45° with the main beam.

7. Less cracks appeared on the beams strengthened with bidirectional fabrics compare to unidirectional fabrics. This may be due to availability of fibre on diagonal compression side causing less stress in concrete face in bidirectional fabrics.
8. Test result reveals that strengthening using bidirectional GFRP sheets had not enhanced the ultimate strength but had increased the ductility of the beam.
9. The angle of twist obtained using ANSYS matches the experimental results for lower range of load value for the beam which are wrapped with GFRP in 90^0 angles with main beam. For higher loads there is a deviation with experimental results for these beams.
10. The experimental results obtained for beams wrapped with GFRP at an angle 45^0 with axis of the beam are in good agreement with ANSYS results.

6.2 SCOPE OF THE FUTURE WORK

This present experimental work can give great scope for future studies. Following areas can be considered for future research:

1. Experimental study on behaviour of flanged RC section wrapped with FRP under combined loading.
2. Effect of different types of FRP like CFRP (carbon fibre reinforced polymer) or hybrid FRP strengthening on torsional behaviour of RC beams.
3. Development of an analytical model to predict full behaviour up to collapse for RC beams strengthens in torsion under combined loading.
4. Developing a non linear finite element model for the analysis of the strengthened rectangular RC Beams using various configurations with different orientation of fibres.

REFERENCES

1. **ACI Committee 440** (1996) State Of Art Report On Fiber Reinforced Plastic
2. **Ameli, M. and Ronagh, H.R.** (2007). “Behavior of FRP strengthened reinforced concrete beams under torsion”, *Journal of Composites for Construction*, **11(2)**, 192-200.
3. **Ameli, M., and Ronagh, H. R.** (2007), “Analytical method for evaluating ultimate torque of FRP strengthened reinforced concrete beams” ,*Journal of Composites for Construction* ,**11**, 384–390.
4. **Amir, M., Patel, K.** (2002).“Flexural strengthening of reinforced concrete flanged beams with composite laminates”,*Journal of Composites for Construction*, **6(2)**, 97-103.
5. **Andre, P., Massicotte, Bruno, Eric**, (1995). “Strengthening of reinforced concrete beams with composite materials : Theoretical study”, *Journal of composite Structures*,**33**,63-75.
6. **Arbesman, B.** (1975). “Effect of stirrup cover and amount of reinforcement on shear capacity of reinforced concrete beams.” MEng thesis, Univ. of Toronto.
7. **Arduini, M., Tommaso, D. A., Nanni, A.** (1997), “Brittle Failure in FRP Plate and Sheet Bonded Beams”, *ACI Structural Journal*, **94 (4)**, 363-370.
8. **Belarbi, A., and Hsu, T. T. C.** (1995). “Constitutive laws of softened concrete in biaxial tension-compression.” *ACI Structural Journal*, **92**, 562-573.
9. **Chalioris, C.E.** (2006). “Experimental study of the torsion of reinforced concrete members”, *Structural Engineering & Mechanics*, **23(6)**, 713-737.

10. **Chalioris, C.E.** (2007a). "Torsional strengthening of rectangular and flanged beams using carbon fibre reinforced polymers – Experimental study", *Construction & Building Materials*, in press (available online since 16 Nov. 2006).
11. **Chalioris, C.E.** (2007b). "Tests and analysis of reinforced concrete beams under torsion retrofitted with FRP strips", *Proceedings 13th Computational Methods and Experimental Measurements (CMEM 2007)*, Prague, Czech Republic.
12. **Chen, J.F. and Teng, J.G.** (2003a). "Shear capacity of fiber-reinforced polymer-strengthened reinforced concrete beams: Fiber reinforced polymer rupture", *Journal of Structural Engineering, ASCE*, **129**(5), 615-625.
13. **Chen, J.F. and Teng, J.G.** (2003b). "Shear capacity of FRP-strengthened RC beams: FRP debonding", *Construction & Building Materials*, **17**, 27-41.
14. **Deifalla A. and Ghobarah A.**(2010), "Full Torsional Behavior of RC Beams Wrapped with FRP: Analytical Model", *Journal of Composites for Construction*,**14**,289-300.
15. **Gobarah,A., Ghorbel, M., and Chidiac, S.** (2002). "Upgrading torsional resistance of RC beams using FRP." *Journal of Composites for Construction* ,**6**,257–263.
16. **Hii, A. K. Y., and Al-Mahadi, R.** (2007). "Torsional capacity of CFRP strengthened reinforced concrete beams." *Journal of Composites for Construction*,**11**,71–80.
17. **Hii, A.K.Y. and Al-Mahaidi, R.** (2006). "An experimental and numerical investigation on torsional strengthening of solid and box-section RC beams using CFRP laminates", *Journal of Composite Structures*, **75**, 213-221.
18. **Hsu, T.T.C. and Mo, Y.L.** (1985). "Softening of concrete in torsional members – Theory and tests", *ACI Journal Proceedings*, **82**(3), 290-303.

19. **Ilki, A. 9K. N., and Koc, V.** (2004). "Low strength concrete members externally confined with FRP sheets." *Structural Engineering and Mechanics*, **18**, 167–194.
20. **Jeng, C.H.** (2010) "Simple rational formulas for cracking torque and twist of reinforced concrete members", *ACI Structural Journal*, **107(19)**, 189–197.
21. **Jeng, C.H. and Hsu, T.T.C.** (2009) "A softened membrane model for torsion in reinforced concrete members", *Engineering Structures*, **31(9)**, 1944–1954.
22. **Kachlakev, D., Miller, T. and Chansawat, K.** (2001). "Finite Element Modeling of Reinforced Concrete Structures Strengthened with FRP Laminates." Final Report, SPR 316, Oregon Department of Transportation-Research Group and Federal Highway Administration, Washington DC.
23. **Karabinis, A.I. and Rousakis, T.C.** (2002). "Concrete confined by FRP material: a plasticity approach", *Engineering Structures*, **24**, 923-932.
24. **Karayannis, C.G.** (2000a). "Smeared crack analysis for plain concrete in torsion", *Journal of Structural Engineering, ASCE*, **126(6)**, 638-645.
25. **Karayannis, C.G.** (2000b). "Nonlinear analysis and tests of steel-fiber concrete beams in torsion", *Structural Engineering & Mechanics*, **9(4)**, 323-338.
26. **Karayannis, C.G. and Chalioris, C.E.** (2000a). "Experimental validation of smeared analysis for plain concrete in torsion", *Journal of Structural Engineering, ASCE*, **126(6)**, 646-653.
27. **Karayannis, C.G. and Chalioris, C.E.** (2000b). "Strength of prestressed concrete beams in torsion", *Structural Engineering & Mechanics*, **10(2)**, 165-180.
28. **Mahmood, M. N. and Mahmood, A. Sh.** (2011) "Torsional behaviour of prestressed concrete beam strengthened with CFRP sheets" 16th International Conference on Composite Structures, ICCS 16

29. **Mitchell, D. and Collins, M. P.** (1974). "Diagonal compression field theory-A rational model for structural concrete in pure torsion." *ACI Struct. J.*, **71**, 396–408.
30. **Onsongo, W. M.** (1978). "Diagonal compression field theory for reinforced concrete beams subjected to combined torsion, flexure, and axial load." Ph.D. thesis, Univ. of Toronto, Toronto.
31. **Panchacharam, S. and Belarbi, A.** (2002). "Torsional behaviour of reinforced concrete beams strengthened with FRP composites", *Proceedings 1st FIB Congress*, Osaka, Japan, 1-10.
32. **Pham, H. B., and Al-Mahaidi, R.** (2004). "Experimental Investigations into flexural retrofitting of reinforced concrete beams using fiber reinforced polymer." *J. Compos. Constr.*, **6**(4), 257-263.
33. **Rahal, K. N., and Collins, M. P.** (1995). "Effect of the thickness of concrete cover on the shear-torsion interaction—An experimental investigation." *ACI Struct. J.*, **92**, 334–342.

Reinforcement For Concrete Structure , ACI 440R-96, American Concrete Institute , Farmington Hills, Michigan
34. **Salom, P.R., Gergely, J.M. and Young, D.T.** "Torsional strengthening of spandrel beams with fiber-reinforced polymer laminates", *Journal of Composites for Construction*, **8**(2), 157-162.
35. **Sause, R., Harries, K. A., Walkup, S. L., Pessiki, S., and Ricles, J. M.** (2004). "Flexural behaviour of concrete columns retrofitted with carbon fibre reinforced polymer jackets." *ACI Struct. J.*, **101**, 708–716.

36. **Tastani, S.P. and Pantazopoulou, S.J.** (2004). “Experimental evaluation of FRP jackets in upgrading RC corroded columns with substandard detailing”, *Engineering Structures*, **26**, 817-829.
37. **Teng, J. G., Chen, J. F., Smith, S. T., and Lam, L.** (2002). FRP strengthened RC structures, Wiley, Chichester, U.K.
38. **Triantafillou, T.C. and Antonopoulos, C.P.** (2000). “Design of concrete flexural members strengthened in shear with FRP”, *Journal of Composites for Construction*, **4(4)**, 198-205.
39. **Vintzileou, E. and Panagiotidou, E.** (2007). “An empirical model for predicting the mechanical properties of FRP-confined concrete”, *Construction & Building Materials*, in press, available online.
40. **Zhang, J. W., Lu, T. Z., and Zhu, H.** (2001). “Experimental study on the behavior of RC torsional members externally bonded with CFRP”. *FRP composites in civil engineering, I*, Elsevier Science, New York.
41. **Zojaji A.R. and Kabir M.Z.** (2011) “Analytical approach for predicting full torsional behavior of reinforced concrete beams strengthened with FRP materials”. *Scientia Iranica A*. **19 (1)**, 51–63